AFML-TR-72-235

EXPERIMENTAL STUDY OF FATIGUE CRACK PROPAGATION AND RETARDATION USING POLYMETHYLMETHACRYLATE

FRANCIS J. PITONIAK, CAPTAIN, USAF

TECHNICAL REPORT AFML-TR-72-235

NOVEMBER 1972

AIR FORCE MATERIALS LABORATORY
AIR FORCE SYSTEMS COMMAND
WRIGHT-PATTERSON AIR FORCE BASE, OHIO

NOTICE

When Government drawings, specifications, or other data are used for any purpose other than in connection with a definitely related Government procurement operation, the United States Government thereby incurs no responsibility nor any obligation whatsoever; and the fact that the Government may have formulated, furnished, or in any way supplied the said drawings, specifications, or other data, is not to be regarded by implication or otherwise as in any manner licensing the holder or any other person or corporation, or conveying any rights or permission to manufacture, use, or sell any patented invention that may in any way be related thereto.

Copies of this report should not be returned unless return is required by security considerations, contractual obligations, or notice on a specific document.

AIR FORCE/56780/14 February 1973 — 300

EXPERIMENTAL STUDY OF FATIGUE CRACK PROPAGATION AND RETARDATION USING POLYMETHYLMETHACRYLATE

FRANCIS J. PITONIAK, CAPTAIN, USAF

FOREWORD

This report was prepared by Captain Francis J. Pitoniak for presentation to the faculty of the School of Engineering of the Air Force Institute of Technology in partial fulfillment of the requirements of the degree of Master of Science. The work was conducted at the Air Force Materials Laboratory under Project 7353, "Research on Metals and Ceramics Leading to Superior Materials for Advanced Air Force System Application," Task Number 735309, "Fundamentals of Failure Mechanisms," with 1st Lt A. F. Grandt, Jr., (AFML/LLP) acting as project sponsor.

This report covers work conducted from September 1971 to September 1972.

The author wishes to express his appreciation to 1st Lt A. F. Grandt, Jr., his thesis sponsor, and to Dr. P. F. Packman, for their initial problem definition and enthusiastic guidance. In addition, the valuable laboratory assistance of Messrs. M. B. Strope, Jr., J. G. Paine, and R. F. Klinger is gratefully acknowledged.

Special thanks is also extended to Major L. T. Montulli, the author's thesis advisor, for his encouragement, timely advice and gentle prodding towards the completion of this work.

This technical report has been reviewed and is approved.

STEVEN A. CRIST, Captain, USAF
Chief, Mechanical Physics Branch
Metals and Ceramics Division
Air Force Materials Laboratory

Abstract

Fatigue cracks were grown in compact tension specimens of polymethylmethacrylate, a transparent polymer which was used as a model for metals. Various peak overloads applied to the constant ΔK baselines used produced changes in the baseline load crack growth rates. One thousand overloads of ΔK = 900 psi $\sqrt{in}$ on a baseline ΔK = 600 psi $\sqrt{in}$ produced a reduced or "retarded" growth rate followed by a net baseline growth rate increase. Five overloads to ΔK = 900 psi $\sqrt{in}$ on a baseline load level of ΔK = 450 psi $\sqrt{in}$ produced apparent crack arrest.

A study of the monochromatic light interference fringe patterns emanating from the fatigue cracks at zero load indicated that the crack surfaces were closed along the saw cut edge and on the free surface of the specimens. The crack surfaces were displaced in the interior of the specimen at zero load. Measurement of the crack opening displacements from the fringe patterns indicated that the crack surfaces opened on the free surface at approximately half the baseline load level for a stress ratio of approximately zero. This is in agreement with the Elber crack closure concept.

TABLE OF CONTENTS

LIST OF ILLUSTRATIONS

LIST OF TABLES

I. Introduction

Accurately predicting the service life of an aircraft structure or, more basically, designing an aircraft for a desired service life is a problem of current concern in the USAF and the civilian aerospace industry. To solve this problem, information in three equally important areas particular to the given structure or design is required. These areas are:

1. The sizes of flaws or cracks actually contained in the structural members or probably present in a future design.
2. The growth rates of these flaws under given conditions.
3. The critical flaw size for catastrophic failure of a given structural member under given loading conditions.

Flaws (referring to item two above) may grow under a constant load (creep) or cyclic load (fatigue) with or without the action of a corrosive environment. This study was concerned with fatigue crack growth with no significant corrosive environment present.

While fatigue crack growth has been under investigation for many years, a complete understanding of the mechanism

by which it occurs has yet to be obtained. Probably the most significant unexplained aspect of fatigue crack growth is the "retardation" observed under variable amplitude loading. Figure 1a shows a typical load spectrum applied to a structural member containing a flaw or crack. The corresponding crack growth due to the cyclic loading or fatigue is shown in Fig 1b . Basic fatigue crack growth laws would predict essentially a smooth crack growth curve but a sharp drop in the crack growth rate is observed immediately after the application of some peak load at cycle n_p. The circled region of reduced crack growth rate has been called "retardation".

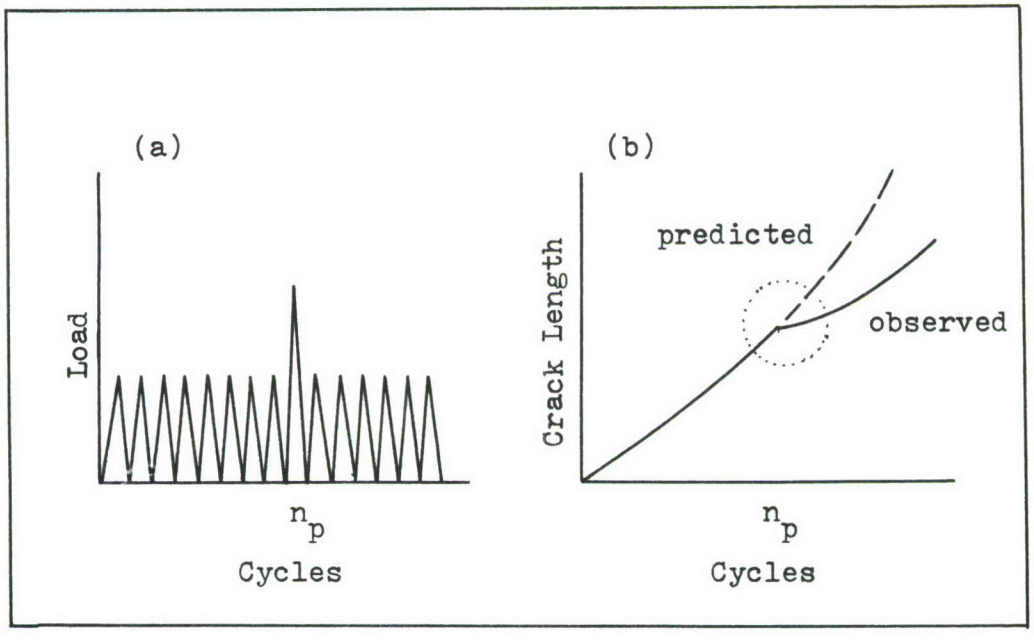

Fig 1. Typical Load Spectrum and Crack Growth.

The specific objectives of the work presented in this paper were:

1. To verify the occurrence of retardation in polymethylmethacrylate (PMMA), a transparent polymer.
2. To characterize this retardation (if it occurred) and compare it to retardation as observed in metals.
3. To study the fatigue crack profiles under various load conditions in an attempt to account for the retardation.

Recent investigations of the retardation phenomenon can be divided into two types. One type primarily has been concerned with generating retardation data on a particular structure material of interest. Retardation data here refers to the amount of retardation obtained from various load spectrums. Emphasis was placed on the experimental determination of an empirical law to predict fatigue crack growth and not on why the retardation occurred. A second type has involved investigations whose primary concern was to explain why retardation occurs. All recent works of this type reviewed by this author have been conducted in metals where only the edge of a crack on a free surface was visible. This limited the type and amount of data obtainable. Only boundary surface observations, which may not be characteristic of conditions in the interior, and post failure examination of the fracture surfaces were possible.

In the present study, a transparent material, PMMA, was used to model fatigue as it occurs in structural metals.

Numerous investigations have shown PMMA to exhibit properties similar to metals when it is subjected to cyclic loading. A few of these include works by Arad, Borduas, Mukherjee and Watts (Refs 2, 3, 11, 18). Being transparent, this material allows observations of the crack on the interior of the specimen and also allows the use of an optical technique (interferometry) to study the shape of the crack surface profile. Many investigators feel that the shape of the crack profile near the tip is an important parameter influencing fatigue crack growth rates (Ref 17).

The following sections contain a brief summary of current information related to this study, a description of the materials and procedures used to conduct this study, and a discussion of the results obtained. A conclusions and recommendations section serves as a summary of the significant findings.

II. Literature Survey

Many of the early investigations of fatigue crack growth in structural materials were conducted on various specimens subjected to constant amplitude cyclic loads. In the literature, the terms "constant amplitude" usually refer to a constant stress intensity factor (K) and that will be the meaning intended in this report. These investigations led to the development of many empirical relations to predict growth rates. The most basic of these relations was formulated by Paris who related the change in the stress intensity factor (ΔK) to fatigue crack growth. In later fatigue investigations under more realistic aircraft type (variable amplitude) load spectrums, the retardation phenomenon was observed when actual growth rates failed to agree with those predicted by the Paris law. In attempts to account for the observed retarded rates, various models have recently been proposed.

In this section, the Paris law, observed retardation characteristics, and current retardation models will be discussed.

Paris Law

The most basic fatigue crack propagation law available today is that formulated by Paris (Ref 21). The Paris law

is stated as

$$\frac{da}{dN} = C\ (\Delta K)^n \qquad (1)$$

where da/dN is the incremental crack growth per cycle of applied load, ΔK is the change in the stress intensity factor at the crack tip during a load cycle i.e. K at maximum stress less K at minimum stress, and C and n are experimentally determined constants for a given material. The law does accurately predict fatigue crack growth rates for constant amplitude (ΔK) loads. However, for variable amplitude loads, the law does not account for any load interaction and predicts higher than observed growth rates if peak tensile loads are applied. The law is still used to provide a first approximation to actual growth rates.

Typical experimental fatigue crack growth data usually is presented on a $\log_{10}$-$\log_{10}$ scale. Figure 2 shows experimentally measured growth rates for PMMA. The constant n is the slope of the curve and C is the $\log_{10}$ da/dN axis intercept. Typical values of the exponent n range from 2 to 6 for most materials.

Retardation Characteristics

While a considerable amount of data has been published on the retardation phenomenon, there has not been full agreement in the results obtained. Some basic qualitative conclusions which do agree are summarized below.

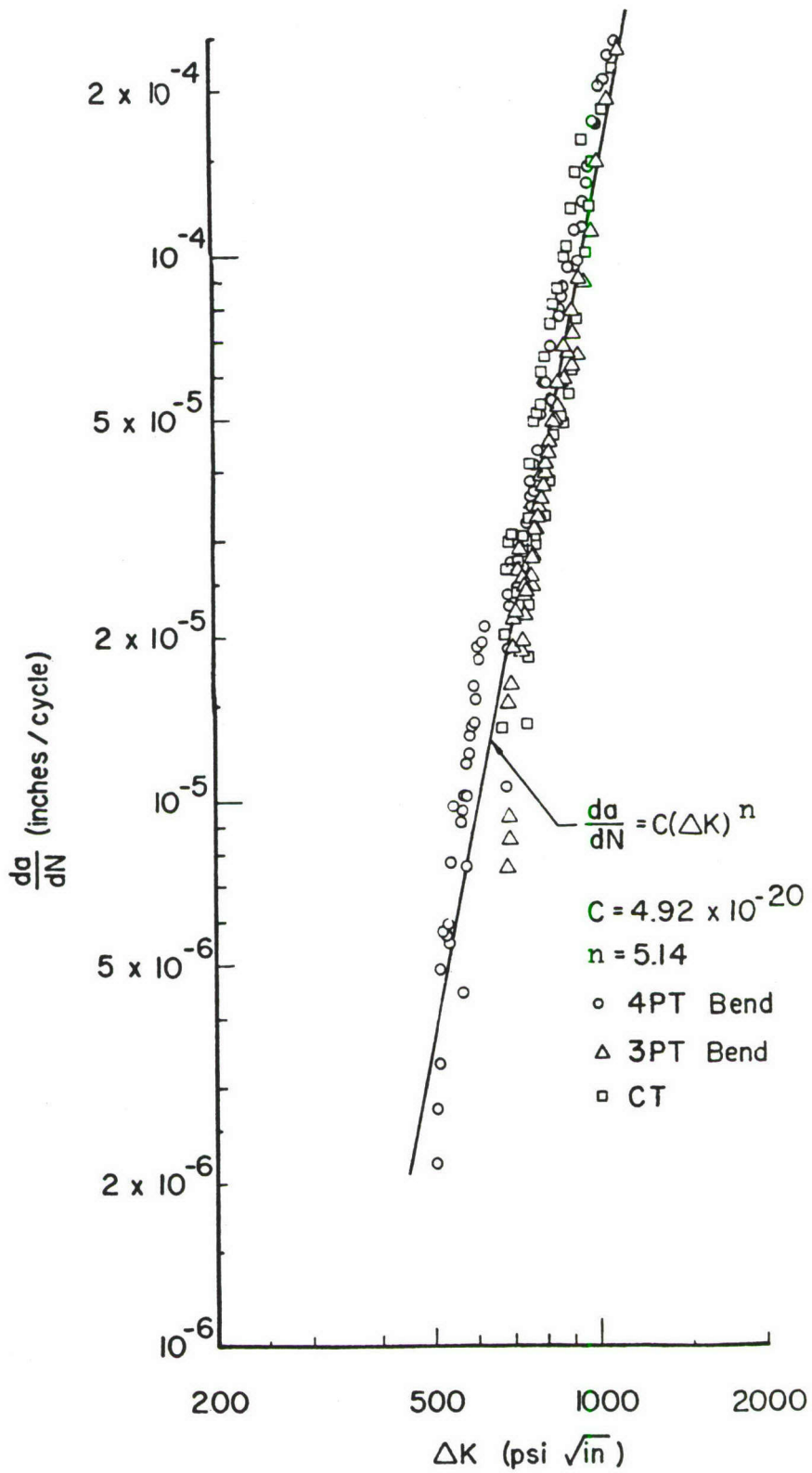

Fig 2. Fatigue Crack Growth Rates for PMMA (Ref 8).

1. For a given baseline ΔK, the amount of retardation observed increases with the magnitude of the overload applied.
2. For a given baseline ΔK, the amount of retardation observed increases to some maximum value with the number of peak loads applied.
3. Complete crack arrest can be obtained for certain values of the baseline ΔK with overloads greater than 100 percent of the baseline.
4. The number of cycles required for a retarded growth rate to return to an unretarded rate is dependent on the maximum amount of retardation incurred. This has been associated with cycles required to grow through the plastic zone created by the peak load.

Retardation Models

Based on experimental observations and intuition, empirical formulas have been developed to predict retarded fatigue crack growth rates (Refs 6, 16, 19, 20). All of these empirical relations are modifications of the basic Paris law, Eq (1). Two of these laws, the Wheeler Model and the Elber Model will be discussed below.

Wheeler Model. The Wheeler model (Ref 19) modifies the Paris equation by including a retardation parameter C_p. The Wheeler equation is given by

$$\frac{da}{dN} = C_p\, C\, (\Delta K)^n \qquad (2)$$

where

$$C_p = \left(\frac{R_y}{a_p - a}\right)^m$$

R_y = current yield zone size

$a_p - a$ = distance from the crack tip to the elastic-plastic interface

m = shaping exponent

Figure 3 illustrates the various quantities used to define the retardation parameter.

Wheeler reasoned that, with the application of an overload on a constant amplitude load spectrum, a large plastic zone is created ahead of the crack tip. During the time that the crack is growing through this plastic zone, the growth should be retarded. The retardation parameter has a minimum value less than unity immediately after a peak load is applied. It increases to unity when the current yield zone reaches the large elastic-plastic interface created by some prior overload. The exponent m provides a means of matching experimental data for various materials.

There are several shortcomings of the Wheeler model. It involves the experimental determination of another exponent m, besides the constants C and n already in the Paris law, and it does not account for the increased retardation with an increase in the number of overloads applied. Only the effect of the largest prior overload is taken into account.

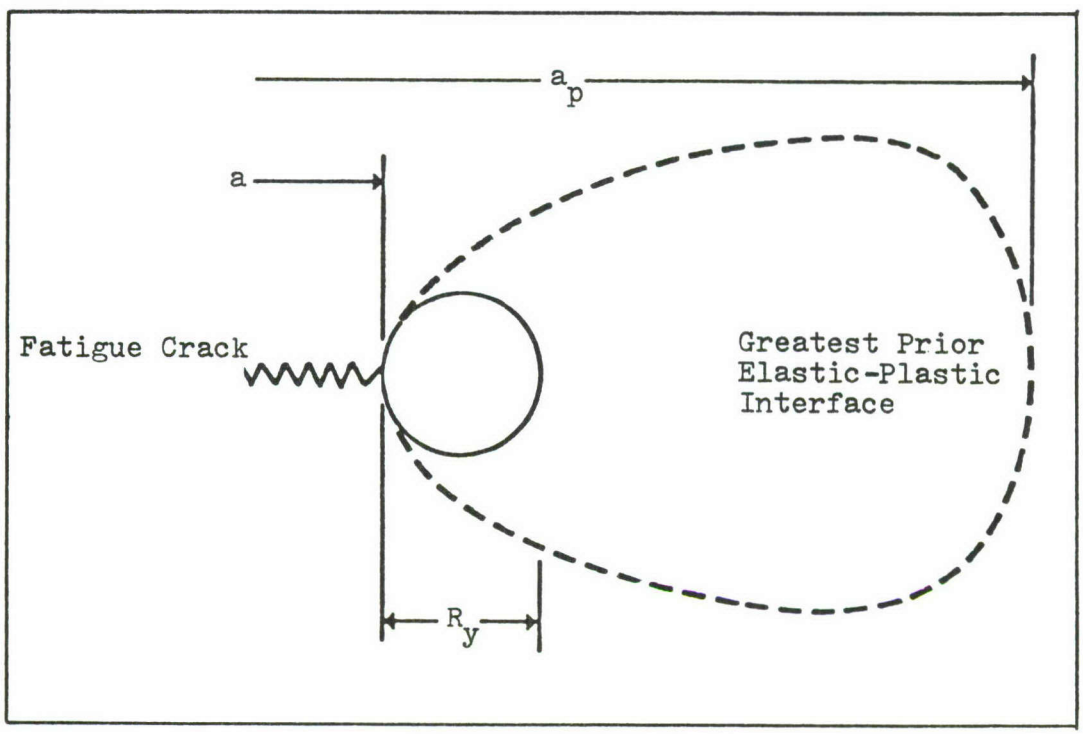

Fig 3. Wheeler Retardation Model.

Elber Model. Formulated from experimental investigations, the Elber model (Refs 6, 7) for retarded fatigue crack growth introduces the concept of crack closure. As a crack propagates through a material, it is surrounded by a zone of plastically deformed material. The material surrounding this plastic region is elastically deformed during the passage of the crack front and, in an attempt to return to zero strain, it creates a compressive stress on the crack surfaces. This compressive stress defined as (σ_{op}) must therefore be subtracted from the far field applied stress

in computing the stress intensity applied to the crack tip. Elber defines the reduced ΔK as ΔK_{eff} and incorporates this into the Paris law as

$$\frac{da}{dN} = C\ (\Delta K_{eff})^n \qquad (3)$$

where $\Delta K_{eff} = U\ \Delta K$

$$U = \frac{\sigma_{max} - \sigma_{op}}{\sigma_{max} - \sigma_{min}}$$

σ_{op} = opening stress level required to overcome the compressive stresses

For a constant ΔK level, σ_{op} and, therefore U would remain constant. For this case, Elber's law would predict a constant growth rate. If an overload is applied to the specimen, a larger plastic zone surrounds the crack tip and increases σ_{op}. This reduces the value of U and, therefore, da/dN. Elber (Ref 6) developed an empirical relation for U from experimental investigations in 2024-T3 aluminum as:

$$U = .5 + .4\ R \qquad (4)$$

where $R = \frac{\sigma_{min}}{\sigma_{max}}$

In this work crack tip stress-displacement measurements were made on the surface of metal specimens during the passage of a crack front and these indicated a two part curve which was accounted for by the opening and closing of the crack surfaces.

Shortcomings of the Elber model are evident. There is currently no way to theoretically calculate U for various materials, and thus experimental investigations must be conducted. Secondly, there is no explanation of how to decrease the value σ_{op} and therefore increase U as the crack grows through the large plastic zone. Essentially, a constant retardation is predicted. Thirdly, there is no way of accounting for the effect of multiple overloads.

III. Experimental Logic and Approach

Logic

The following reasoning was used by the author in the conduct of this investigation. The energy required for fatigue crack growth is supplied by the far field applied loads on a body. Knowledge of how this energy is made available to or distributed around the crack tip during a load cycle is very critical to understanding the fatigue process. This energy can be defined in terms of stress and strain with no loss in generality and this is what the concept of the stress intensity factor (K) attempts to do. The stress intensity factor determines the magnitude of the stresses at the crack tip and is a function of the specimen geometry, the far field applied loads, and the crack length. One drawback of the stress intensity is that it assumes an "ideal" mathematically defined crack geometry which does not change from cycle to cycle. While the crack shape during constant amplitude fatigue would not be "ideal", it would not change from cycle to cycle and, therefore, a constant growth rate as predicted by the Paris equation would be valid. During a variable amplitude test, the crack shape should change and produce second order fatigue effects. Retardation is just such a second order effect.

A study of fatigue crack growth and, in particular, retardation should involve a study of the crack tip changes. Two questions immediately arise, however. On how small a scale must one look for these changes and how near the crack tip are these changes important? Elber and Adams (Refs 6, 1) have attempted to measure changes of crack opening displacements (COD) on the surface of metal specimens during the passage of a crack. While they were limited in the scale of their measurements, valuable information was obtained indicating a crack closure phenomenon.

The use of a transparent material in this study was prompted by the ability to use interference of light to make small measurements (order of 10^{-5} inches) in the fatigue crack profile.

Approach

The first stated objective of this study was to verify that some form of retardation occurred in PMMA. To accomplish this, fatigue cracks were grown at a constant ΔK in compact tension (CT) specimens of PMMA with the crack front photographed periodically to determine baseline growth rates. Then, overloads were applied to the specimens and growth rates immediately after the application of these peaks were compared to the baseline rates obtained previously. The characteristics of the retardation were compared to those of the retardation occurring in metals to verify that PMMA was a suitable model. Once this fact was established, a study of the interference fringe patterns obtained from the

fatigue cracks was conducted.

PMMA exhibits viscoelastic, i.e., time dependent, properties. Thus, it was necessary as a secondary objective of the interferometry study to determine what effect stress relaxation would have on the fringe pattern of a fatigue crack. From this study, a "relaxed" reference state could be established from which zero load fringe pictures could be compared.

IV. Experimental Materials and Apparatus

A description of the materials and apparatus used during the course of this study follows. The steps used in accomplishing the study with the present materials will be discussed in the procedure section.

Tensile Test Specimen

Figure 4 shows the tensile test specimen used in this study. The specimens were fabricated out of polymethylmethacrylate (PMMA). The PMMA used was a standard grade unshrunk Plexiglas sheet from the Rohm and Haas Company.

Compact Tension Specimen

The specimen chosen for the fatigue crack retardation study is known as the compact tension (CT) specimen. Commonly used for K_{Ic} measurements, this specimen has been proposed as a standard fracture toughness testing specimen by the American Society for Testing and Materials (ASTM). Its compact size and shape made it very suitable for the present study. Figure 5 gives the geometry, dimensions and stress intensity calibration for the specimens used. These specimens were fabricated from the same sheet of material as the tensile test specimens.

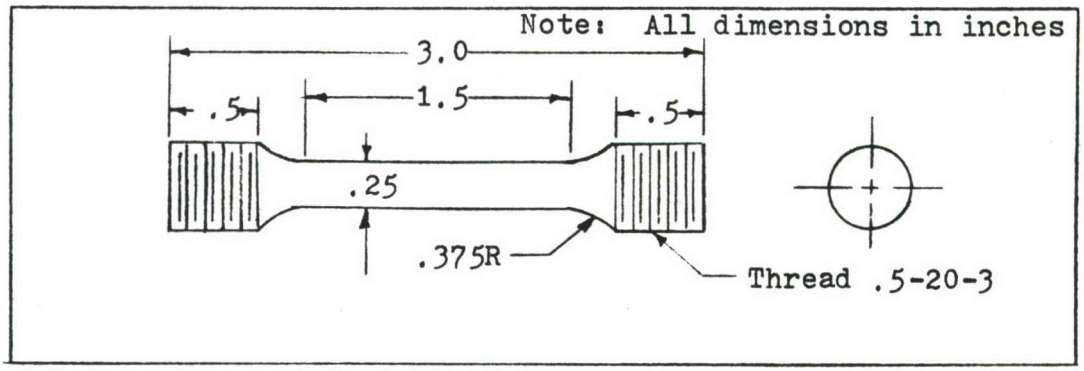

Fig 4. Tensile Test Specimen

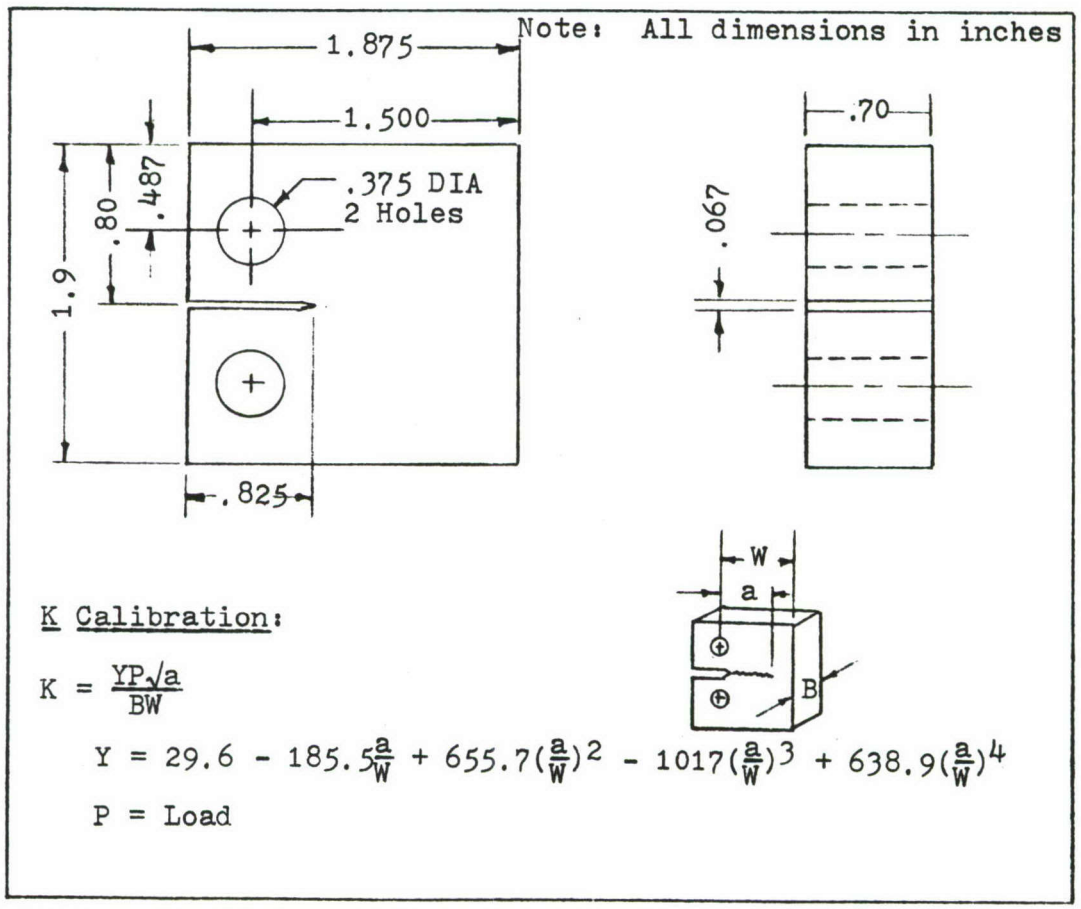

K Calibration:

$$K = \frac{YP\sqrt{a}}{BW}$$

$$Y = 29.6 - 185.5\frac{a}{W} + 655.7\left(\frac{a}{W}\right)^2 - 1017\left(\frac{a}{W}\right)^3 + 638.9\left(\frac{a}{W}\right)^4$$

P = Load

Fig 5. Compact Tension Specimen.

Loading Apparatus

An MTS (5000 lb capacity) electrohydraulic fatigue testing machine was used to initiate and grow fatigue cracks under the various load spectrums. This machine was capable of loading specimens at various frequencies with continuous control of the load applied to the specimen. The load could be applied in various functions (sinusoidal, ramp, square wave etc.). Figure 6 shows the arrangement used to grow the fatigue cracks and photograph the crack front progress.

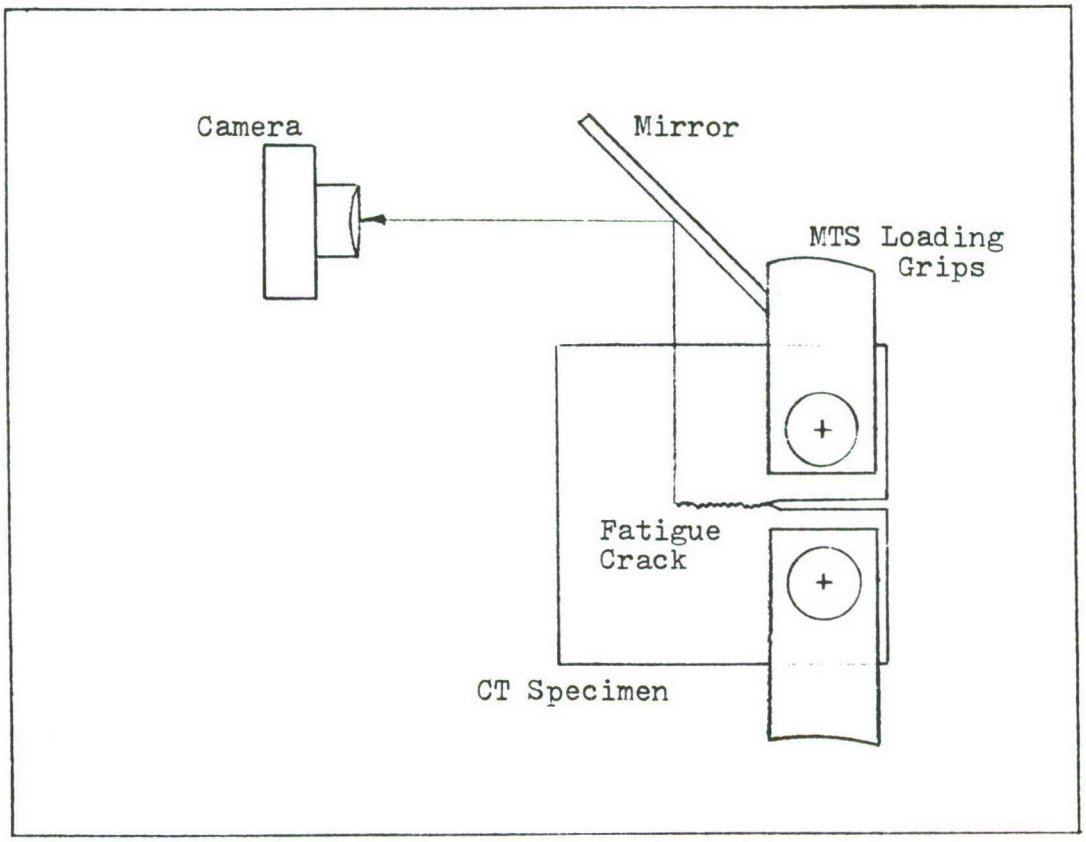

Fig 6. Loading Arrangement.

Monochromatic Light Source

A sodium arc lamp was used as the monochromatic light source for the interferometry study. The light had a wavelength of 5890 angstroms or 2.32×10^{-5} inches.

V. Experimental Procedures

Baseline Tests

To provide baseline information on the material used in this study, a series of tensile tests was conducted to obtain stress-strain data and yield strength. These tests were run on an Instron machine at four different strain rates using the tensile specimen previously described. An extensometer with a one-inch gage length was used to make strain measurements.

K_{Ic} measurements were also made on the Instron machine. Precracked CT specimens previously described were used for these measurements.

Constant amplitude (ΔK) growth rate data was obtained from the constant load portion of the retardation tests described later. This data was compared to data published by other investigators.

Retardation Study

All of the CT specimens used in this study were machined from the same sheet of Plexiglas (nominally .7 inches thick) with the same directional orientation to assure uniform mechanical properties among the specimens. Then, the sides of the specimens were polished to allow photography of the crack profile from the top of the specimen. All

specimens were also annealed by placing them in an oven at 102°C for 24 hours followed by a cooling period to room temperature of 24 hours. The annealing was accomplished to remove any residual stresses left in the material by the machining process. The testing environment was uncontrolled.

Fatigue cracks were initiated from a scalpel cut placed in the V notch previously machined in the specimen. To reduce crack initiation time, the load during initiation was kept high (ΔK ranging from 700 to 900 psi $\sqrt{in}$). Fatigue cracks would typically start at several areas along the notch in 5000-10000 cycles. These small cracks were allowed to grow and join to a uniform crack front through the thickness of the specimens before any growth data was obtained. All tests except one were conducted at a frequency of 3 cps with the load applied in a sinusoidal fashion. Work by Arad, Mukherjee and Hertzberg (Refs 1,12,9) have indicated that no significant crack tip thermal heating occurred at frequencies less than 5 cps.

Baseline ΔK's of 450, 550, 600 psi $\sqrt{in}$ were used with peak loads to 750 and 900 psi $\sqrt{in}$. Table I (in the Results section, page 29) shows the test conditions for each run. During the conduct of each test, the actual load applied to the specimen had to be reduced as the crack grew to keep the constant ΔK desired for each test. The load was lowered at crack growth increments of .01 inches. This procedure allowed a constant $\Delta K \pm 15$ psi $\sqrt{in}$ to be applied to each specimen.

Since a small preload (nominally 5 lbs) was required on the MTS machine to ensure the stability of the programmed positive sine wave loading function, the stress ratio ($R = \sigma_{min}/\sigma_{max}$) varied from .05 to .1. Its change during a test was not considered significant.

The crack front was photographed at periodic intervals to provide a permanent record of the crack growth during the load spectrum. Typically, baseline growth rates were obtained over a period of 10,000 cycles prior to the application of a single or multiple peak load(s). This initial baseline period allowed the cracks to grow out of the possible retardation effects of the high ΔK loads used during the crack initiation. The tests were continued for an additional 10,000 cycles to ensure a uniform growth rate had been established again.

A 35 mm camera was used with a set of bellows to allow approximately a 1:1 image size on the photographic negative obtained. When viewed through a slide projector, a final magnification of about 25 to 1 could be obtained. Crack growth to .001 inches could be measured easily in this manner.

Interferometry Study

Interference fringe photographs of the fatigue crack profiles were obtained from the specimens used in the retardation study. The photographs were obtained by subjecting the fatigue cracked specimens to a sodium-arc light source as shown in Fig 7. When the displacements between the upper and lower surfaces of the crack differed by an odd number of

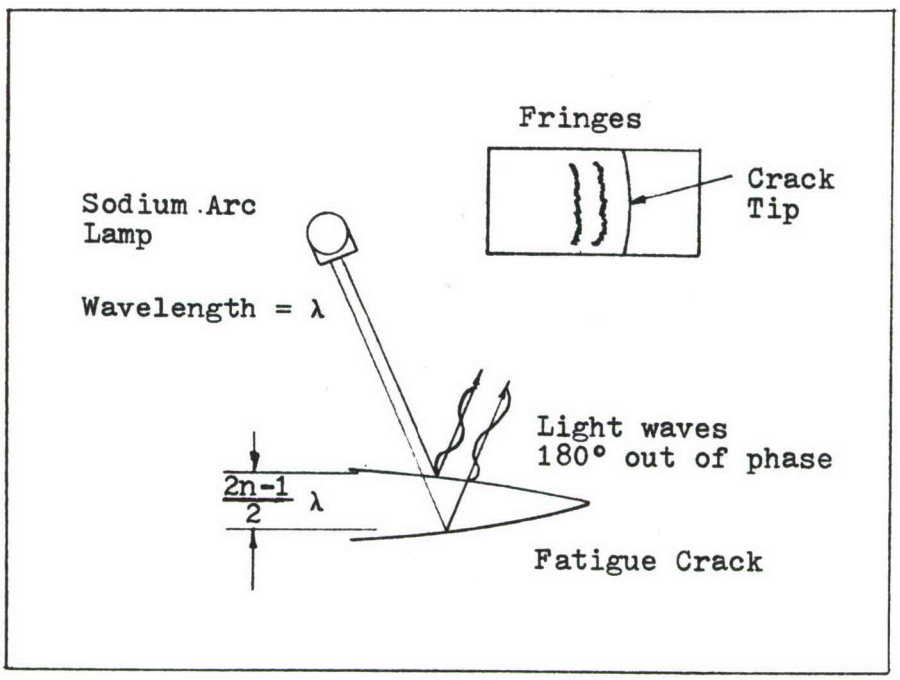

Fig 7. Interferometry Arrangement.

half wavelengths of the light, individual light waves reflecting from the crack surfaces would destructively interfere and produce a shadow or fringe. In this manner, the displacements essentially could be mapped from the photographs taken.

Three studies were made from the fringe patterns obtained. Several specimens were dead weight loaded in a tensile and compressive cycle. Fringe pictures were taken at load increments of 2.5 lbs. These photographs were used to obtain the corresponding changes in the crack profiles during load cycles.

In a second study, series of fringe photographs were taken at varying time intervals after a cracked specimen was

removed from the MTS machine. These were used to study the crack profile changes with stress relaxation.

A third study compared fringe patterns of fatigue cracks with different load histories. This also included a comparison of fringe patterns obtained before and after the applications of overloads.

VI. Results and Discussion

Material Properties and Baseline Data

Stress-strain curves for the PMMA used in the test annealed condition are shown in Fig 8. Four different strain rates are shown. The PMMA behaved linearly up to about 4000 psi for the three faster strain rates. At the .00002 in/in/sec strain rate, the viscoelastic nature of this material was quite apparent. An average .2 percent yield strength (σ_y) was measured as 7000 psi. This compares well with other published data.

The values of the critical stress intensity factor (K_{Ic}) obtained ranged from 930 to 1050 psi $\sqrt{in}$. The crack growth rates for the constant ΔK portions of the retardation tests are shown in Fig 9 as a function of the baseline ΔK. A log-log scale is used. These growth rates compare well with other published data.

Visual macroscopic observations of the crack surfaces indicated a "rough" type of growth occured at load levels above ΔK = 600 psi $\sqrt{in}$. At levels below ΔK = 600 psi $\sqrt{in}$, there was a transition to a very "smooth" fatigue growth as shown in Fig 10. It was very easy to identify the region of application of peak loads in this manner.

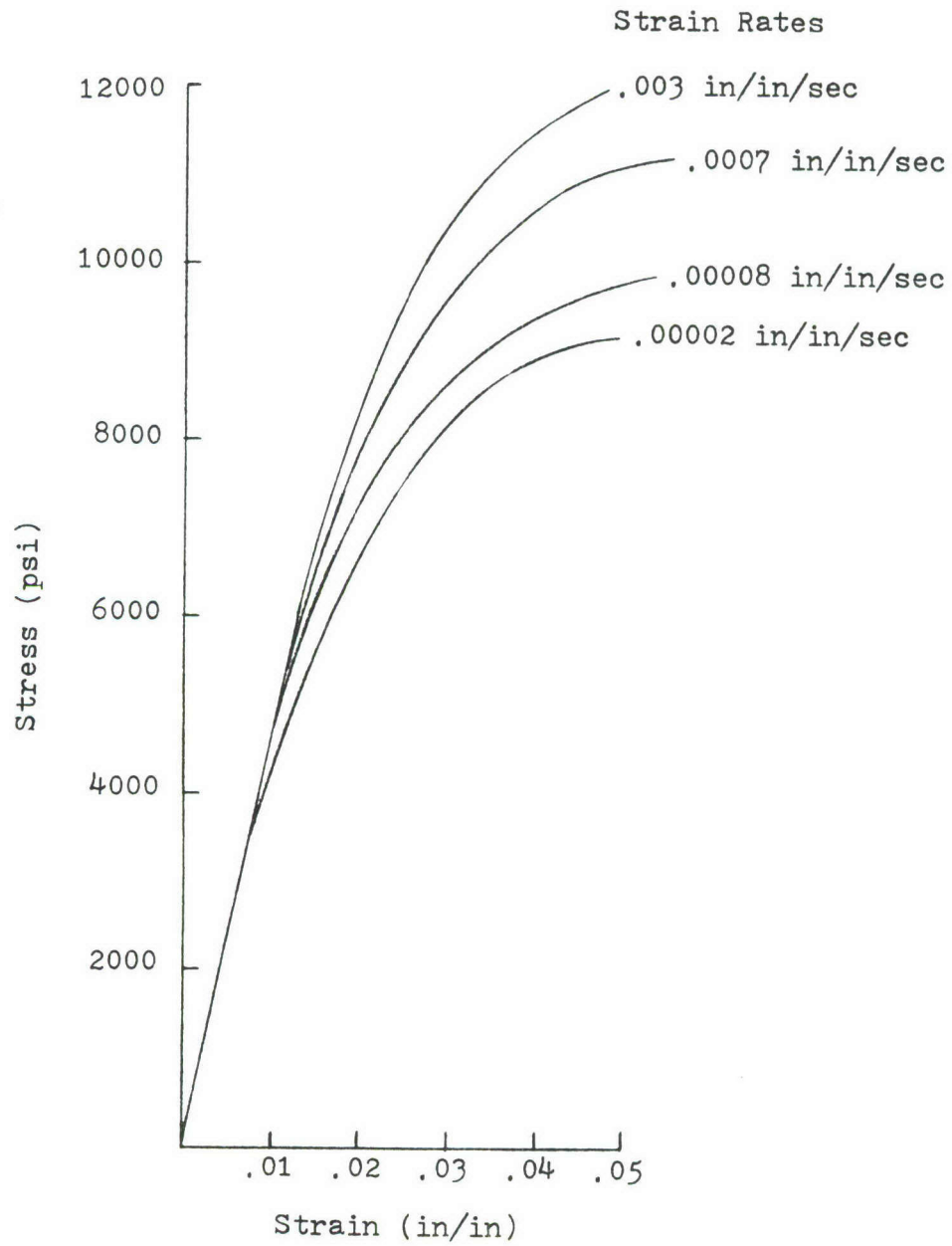

Fig 8. PMMA Stress-Strain Data.

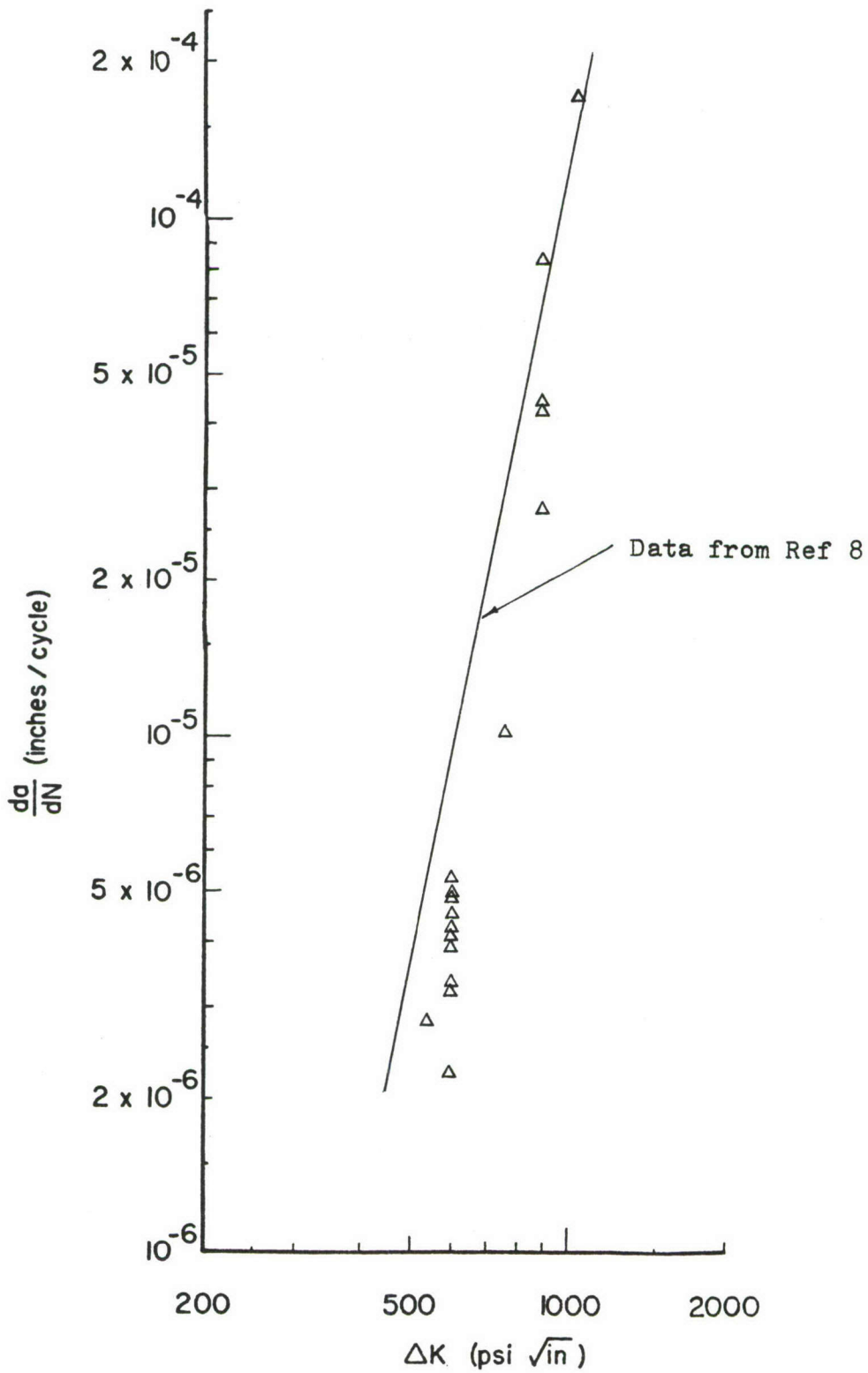

Fig 9. PMMA Fatigue Crack Growth Rates.

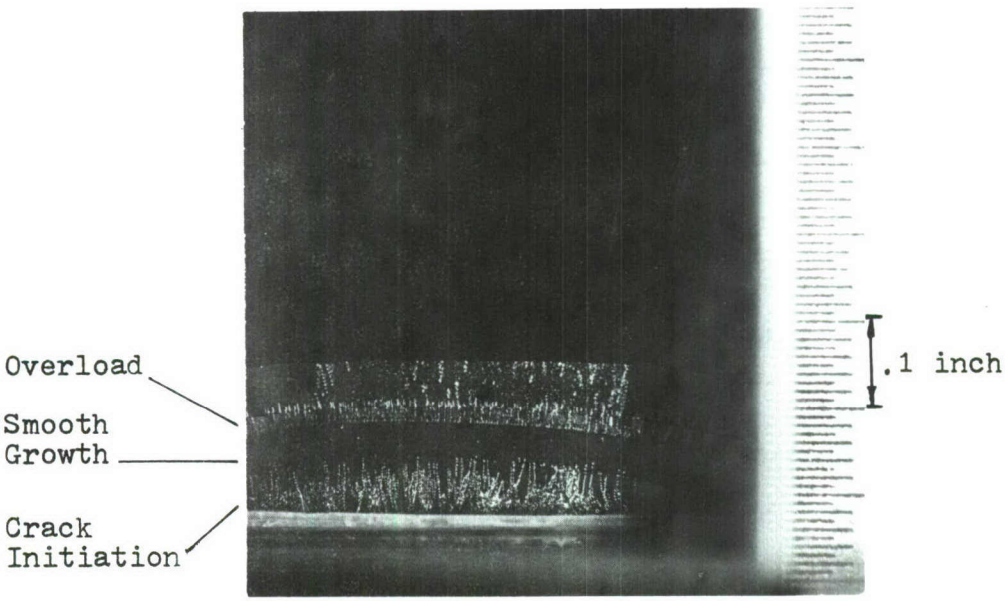

Fig 10. Fatigue Crack Surface Appearance.

In general, the fatigue crack front on the surface of the specimen lagged behind the crack front in the center of the specimen. This is probably associated with the transition from the plane stress conditions on the surface to the plane strain conditions in the interior of the specimen. Approximately 70 percent of the crack front was considered to be in plane strain conditions based on these observations.

Retardation Data

The fatigue crack growth rates for the CT specimens tested are summarized in Table I along with the load conditions, and the initial and final crack lengths. The

Table I

Summary of Retardation Tests

Specimen Data			Load History			Growth Rates (10^{-5} in/cy)			
No.	Initial Crack Length (in)	Final Crack Length (in)	Baseline ΔK (psi $\sqrt{in}$)	Overload ΔK (psi $\sqrt{in}$)	No. of Overloads	Initial Baseline	Overload	Retarted Rate	Final Baseline
106	.61	.63	600	- - -	0	.23	- - -	- - -	- - -
20R	.65	.70	600	- - -	0	.49	- - -	- - -	- - -
22R	.59	.63	600	- - -	0	.34	- - -	- - -	- - -
23R	.66	.70	600	- - -	0	.43	- - -	- - -	- - -
28	.60	.70	600	-	0	.32	-	-	-
110	.60	.71	600	750	1	.35	-	.35	.35
104*	.64	.79	600	900	1	1.48	-	.77	.90
111	.58	.71	600	900	1	.41	-	.23	1.21
114	.60	.71	600	900	1	.34	-	.42	.53
117	.62	.75	600	900	1	.54	-	.58	.81
118	.61	.78	600	900	1	.50	-	.68	1.30
20	.55	.65	600	900	10	.40	-	.28	.64
22	.53	.59	600	900	10	.20	-	.23	.43
23	.57	.66	600	900	10	.31	-	.30	.61
27	.60	.70	600	900	10	.41	-	.32	.37
24	.54	.64	600	900	100	.45	-	.34	.70
25	.54	.66	600	900	100	.39	-	.25	.46
26	.54	.61	600	900	100	.24	-	.16	.25
108	.65	1.02	600	900	1400	-	4.36	.20	1.55
115	.65	.84	600	900	1400	-	8.27	.17	.81
116	.57	.68	600	900	1600	-	4.15	.19	.43
107	.60	.66	550	900	1000	-	2.69	.10	.29
112	.63	.72	600	750	3000	-	1.05	.21	.50
107R	.66	.69	450	900	5	.073	-	0	0
30	.57	.62	450/ 500	-	0	.045	-	-	-

*Test terminated prior to reaching final baseline rate.
Test conducted at 1 cps.

initial baseline rates listed were the constant growth rates measured before an overload(s) was applied as shown in Fig 11. The retardation rates listed were the rates averaged over .003 inches of crack growth after the overload was applied. No initial baseline rates were measured for the tests where 1000 or more overloads were applied; however, the rate during the application of the overloads was measured. The final baseline rates were the final rates measured at the end of each test.

One, 10, and 100 Overloads. All of the following tests discussed had a baseline ΔK = 600 psi $\sqrt{in}$. A single overload to ΔK = 750 psi $\sqrt{in}$ produced no measureable retardation or effect on the baseline rate. Single as well as 10 and 100 overloads did produce measureable effects on the baseline growth rates but there was no significant difference in the three cases. A typical growth curve is shown in Fig 12. During the 600 to 800 cycles following the overload, no growth or very small increments (less than .001 inches) were measured. Following this, there was a rapid return to a final baseline rate. Because the region of significant reduced growth was so small, it was felt that a more meaningful growth rate to measure would be the average over the growth increment equal to the theoretical plastic zone size (R_y). This may be calculated as

$$R_y = \frac{1}{2\pi} \left(\frac{K_{max}}{\sigma_y} \right)^2 \qquad (5)$$

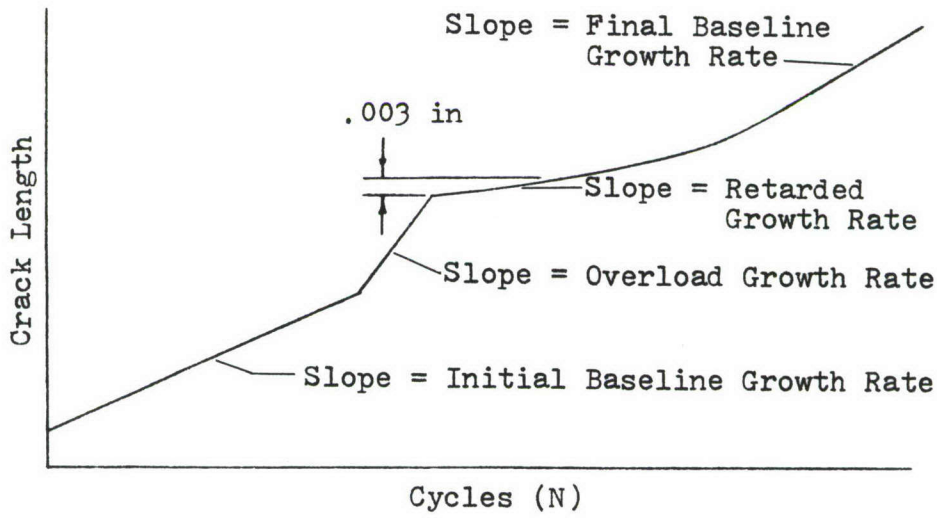

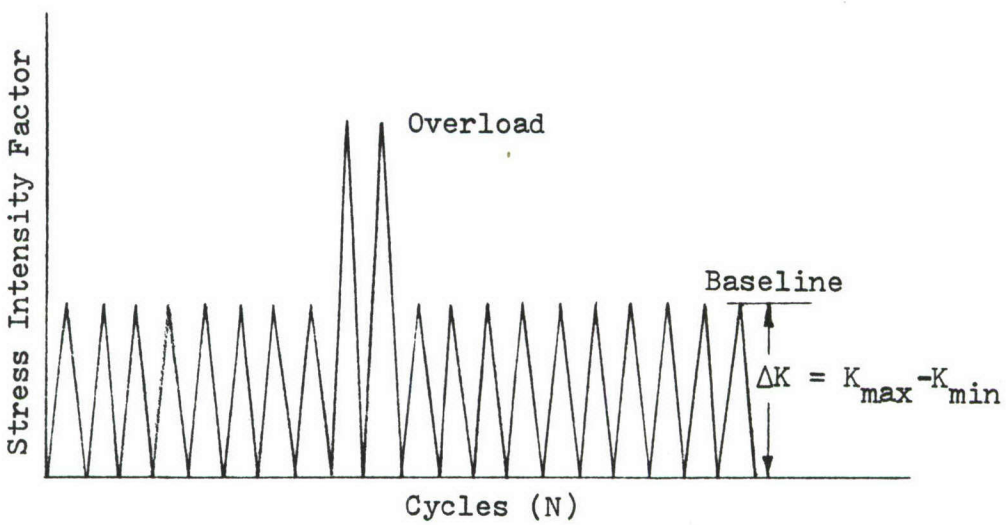

Fig 11. Typical Test Load Spectrum and Crack Growth Rates.

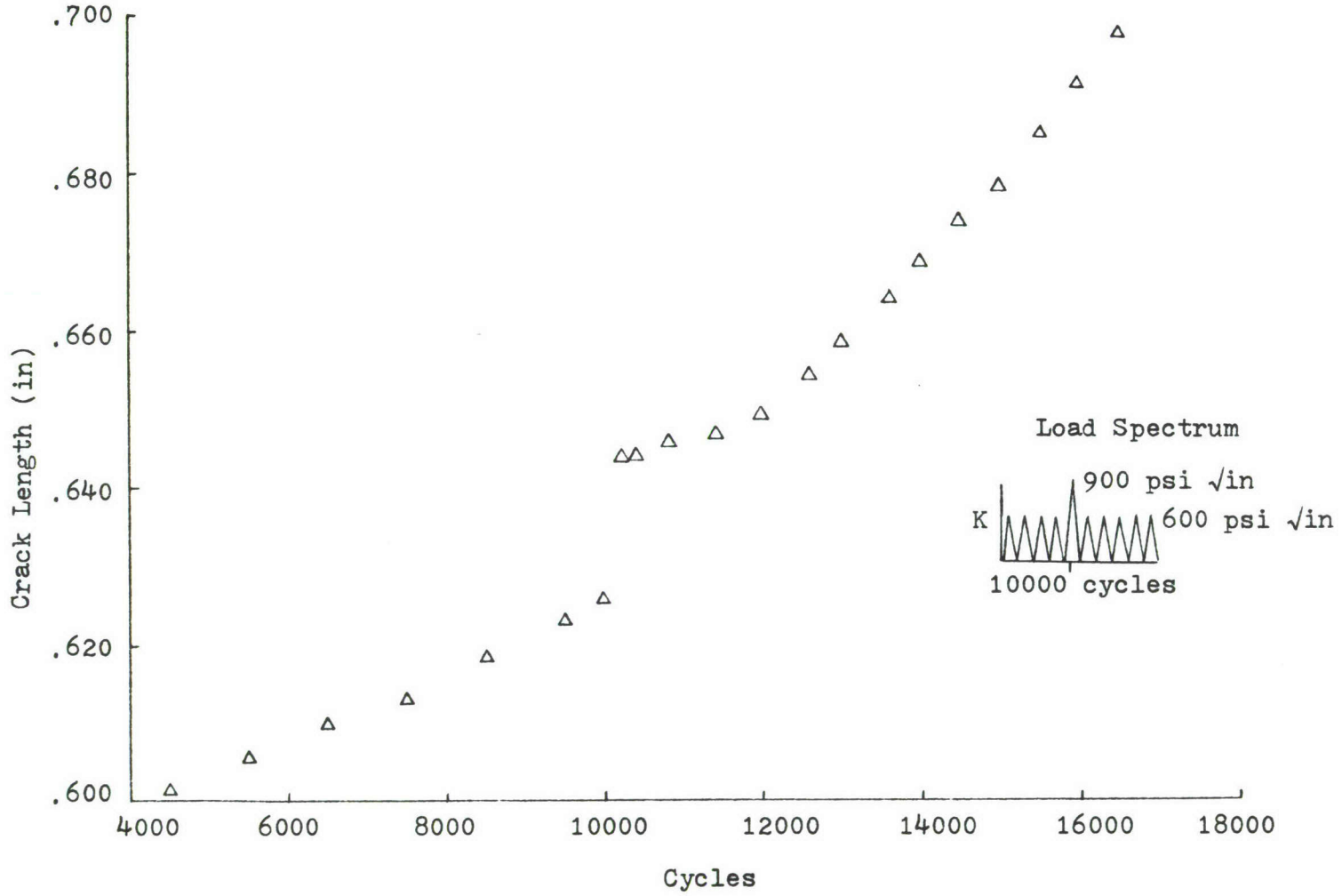

Fig 12. Retarded Crack Growth for Test 111.

One must assume an average yield stress σ_y based on some average strain rate at the crack tip. Using σ_y of 7000 psi, R_y equals approximately .003 inches.

In some cases the average growth rate measured over this distance was greater than the initial baseline rate. In all cases, however, this average retarded rate was smaller than the final baseline rate. At this baseline (ΔK = 600 psi $\sqrt{in}$) it appears that the most significant effect of an overload to ΔK = 900 psi $\sqrt{in}$ is a net baseline rate increase and that the "retardation", while measureable, was insignificant to the total specimen life.

A significantly higher initial baseline growth rate was measured for test 104 which was conducted at a slower frequency (1 cps compared to 3 cps for all other tests). This is in agreement with a conclusion of Mukherjee (Ref 11) that over a limited range of frequencies, fatigue crack growth rates in PMMA increase with a decrease in frequency.

Tests 20R, 22R, and 23R. To further investigate the baseline growth rate increase discussed above, three tests were partially repeated. After allowing the specimens used for tests 20, 22, and 23 to stress relax for two weeks, the same previously applied baseline loads of ΔK = 600 psi $\sqrt{in}$ were applied to the specimens (tests 20R, 22R, and 23R). Table II shows the average growth rates for tests 20R, 22R, and 23R compared with the average initial baseline growth rate, retarded growth rate and final baseline growth rate of tests 20, 22, and 23.

Table II

Comparison of Tests 20, 22, and 23 with Tests 20R, 22R and 23R (Rates x 10^{-5} in/cy).

	Initial Baseline Growth Rate	Retarded Growth Rate	Final Baseline Growth Rate
Average for Tests 20, 22, and 23	.30	.27	.56
Average for Tests 20R, 22R, and 23R	.42		

The average baseline growth rate for the repeated tests was significantly lower than the average for the final baseline growth rates previously measured.

It appears, therefore, that the stress relaxation has allowed the ΔK = 600 psi $\sqrt{in}$ baseline growth rate to return nearer to the original initial baseline growth rate. This indicates that the overloads are in fact responsible for the baseline rate increase.

1000 or More Overloads. The effect of an "infinite" number of overloads was approximated by applying 1000 or more overloads in certain tests. These tests did produce a significant amount of retardation besides producing a baseline increase as observed in the one, 10, and 100 overload tests. Tests 108, 115, and 116 with baseline and overload ΔK values of 600 and 900 psi $\sqrt{in}$ respectively exhibited reduced growth over crack growth increments up to .015 inches. A typical growth curve (that for test 116) is shown in Fig 13. The average retarded rate for this case was

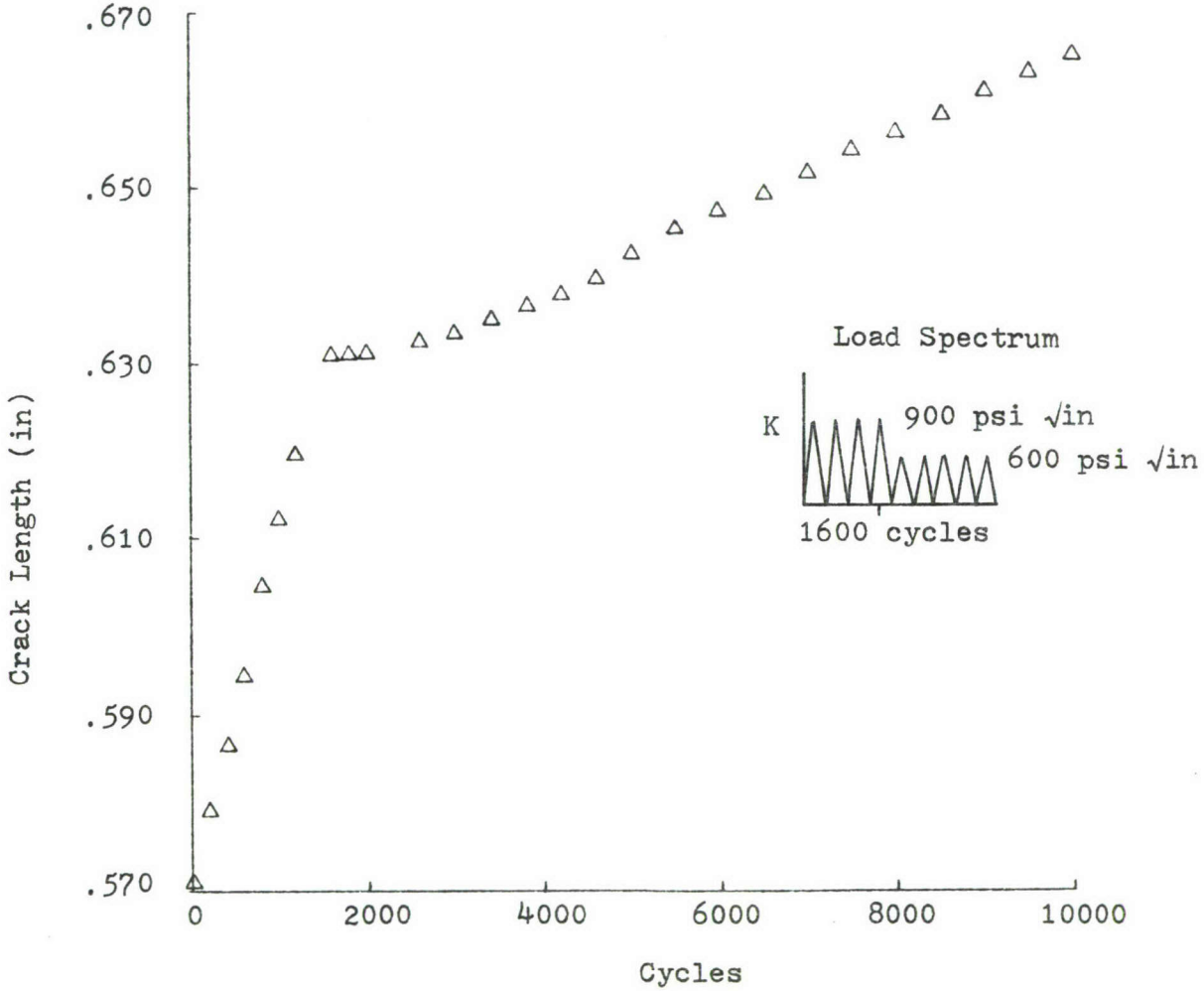

Fig 13. Retarded Crack Growth for Test 116.

$.19 \times 10^{-5}$ in/cy which is significantly less than the average initial baseline rate of $.28 \times 10^{-5}$ in/cy and the average retarded rate of $.37 \times 10^{-5}$ in/cy for the one, 10, and 100 overload tests.

Tests 107 and 112 (Table I) show the effect of the baseline ΔK and the magnitude of the overload ΔK. Overloads to $\Delta K = 750$ psi $\sqrt{in}$ produced less retardation than overloads to $\Delta K = 900$ psi $\sqrt{in}$. An overload value of $\Delta K = 900$ psi $\sqrt{in}$ produced more retardation on a lower baseline of $\Delta K = 550$ psi $\sqrt{in}$ ($.1 \times 10^{-5}$ in/cy compared to an average value of $.19 \times 10^{-5}$ in/cy for a baseline $\Delta K = 600$ psi $\sqrt{in}$).

Tests 107R and 30. Test 107R shows an example of crack arrest. The test was stopped 35,000 cycles after the application of 5 overloads to $\Delta K = 900$ psi $\sqrt{in}$ when no measureable crack growth was observed during this period. Test 30 was an attempt to repeat the test conditions of test 107R. It was found, however, that sustained crack growth could not be maintained at $\Delta K = 450$ psi $\sqrt{in}$. It appears that $\Delta K = 450$ psi $\sqrt{in}$ for a $R \approx 0$ is approaching a lower limit of producing fatigue crack growth. The behavior of this specimen will be discussed in more detail later in this report in relation to observed crack opening displacements.

Discussion. In general, overloads were found to have an effect on constant ΔK crack growth rates in PMMA. This effect was dependent on the value of the baseline ΔK. At a baseline of $\Delta K = 450$ psi $\sqrt{in}$, no measureable growth was

observed in 35,000 cycles with 5 overloads to ΔK = 900 psi $\sqrt{in}$ while, at a baseline of ΔK = 600 psi $\sqrt{in}$, 1000 or more overloads to ΔK = 900 psi $\sqrt{in}$ were required to produce any significant amount of retardation. This observation is in some aggreement with work by other investigators.

Corbley and Packman (Ref 4) conducted a retardation investigation in 7075-T6511 aluminum CT specimens. They used baselines of ΔK = 5, 10, and 15 ksi $\sqrt{in}$ with overloads to ΔK = 10, 15, 20, 23, and 25 ksi $\sqrt{in}$. They observed crack arrest with 100 percent overloads to ΔK = 10 ksi $\sqrt{in}$ on a baseline of ΔK = 5 ksi $\sqrt{in}$. At a baseline of ΔK = 10 ksi $\sqrt{in}$, however, overloads to ΔK = 23 ksi $\sqrt{in}$ did not produce crack arrest. Crack growth at lower values of the baseline were found more sensitive to overloads.

The increase in the baseline crack growth rate observed in this study is unexplained at this time. A somewhat similar observation was made by James (Ref 10). In his work in type 304 stainless steel, fatigue crack growth rates were measured as a fatigue crack progressed through a weldment in the specimen. The crack growth rate decreased as the crack approached the heat affected zone caused by the welding process and then increased above the initial rate as the crack grew out of the weld. James attributed the decrease first observed to compressive stresses left in the material by the welding process. He also reasoned that the stresses ahead of the crack tip had to redistribute themselves as the crack grew through the region of compressive stresses creating traction free surfaces. Exactly how this redistribution of

stresses occured and how they affected the crack growth rate was unexplained.

Interferometry Data

Load Cycle COD Measurements. This section contains a series of interference fringe patterns photographed from CT specimen fatigue cracks under various load conditions. Specific observations will be noted from the photographs followed by a discussion of the interpretation of the fringe patterns. Plots of the actual crack profiles during a tension and compression load cycle also are shown in this section.

Before beginning the discussion, however, it will be necessary to illustrate certain terms to be used and orient them in relation to the CT specimen. Figure 14 shows a CT specimen containing a fatigue crack and the three types of crack profiles shown later in this section.

The fringe photographs were taken looking down on the XZ plane. The three crack profiles obtained from each fringe pattern are called the center profile, surface profile and the saw cut profile as illustrated.

(Tensile Cycle). Figures 15 and 16 show the corresponding fringe patterns of a CT specimen fatigue crack under seven different loads. Several other series of such photographs are shown in Appendix B. While the exact number of fringes and fringe shapes in each series of photographs varied between specimens depending on the crack length and

the load history, the same general types of patterns were observed. The following results and discussions therefore will be considered typical to fatigue cracks in PMMA grown under similar conditions.

The following sequence of observations was noted as tensile load was increased on the specimen.

1. At zero load, the fringe pattern consists of symmetric concentric "racetrack" shaped closed lines (Fig 15, Load = 0 lbs).

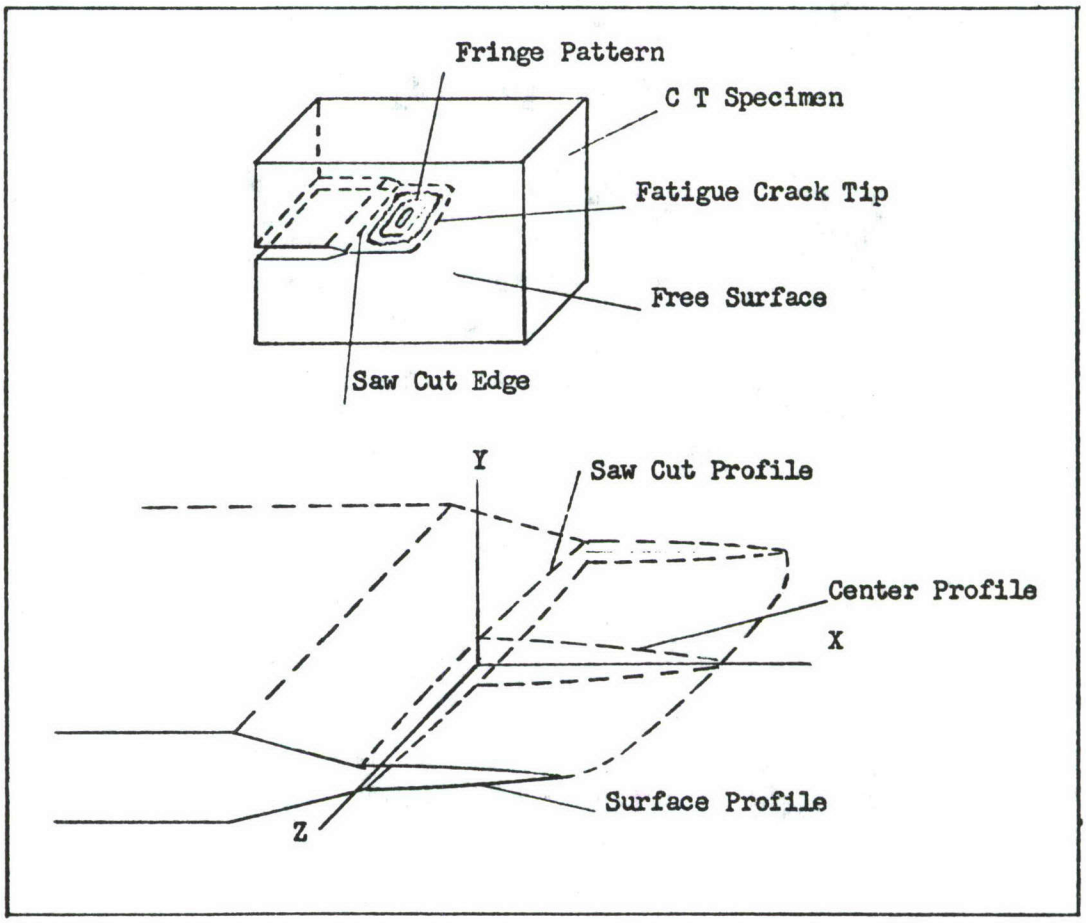

Fig 14. Fatigue Crack Profiles and Orientation.

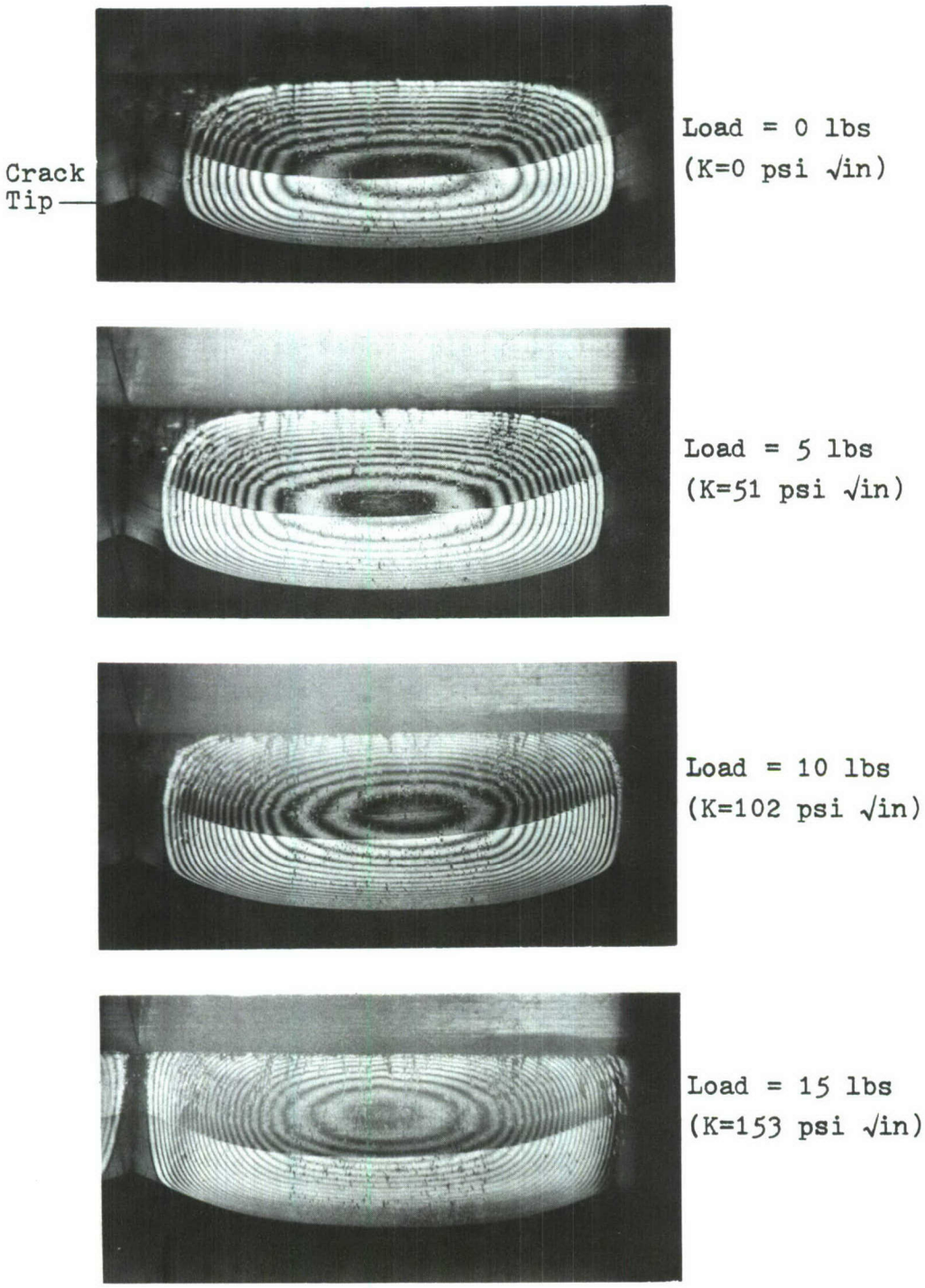

Fig 15. Specimen 28 Fringe Patterns at Tensile Loads of 0, 5, 10, and 15 Pounds.

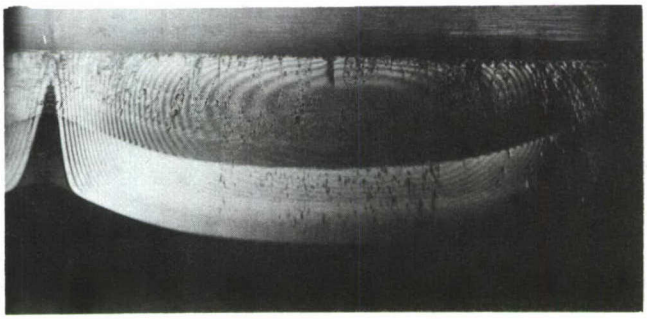

Load = 17.5 lbs
(K=178 psi $\sqrt{in}$)

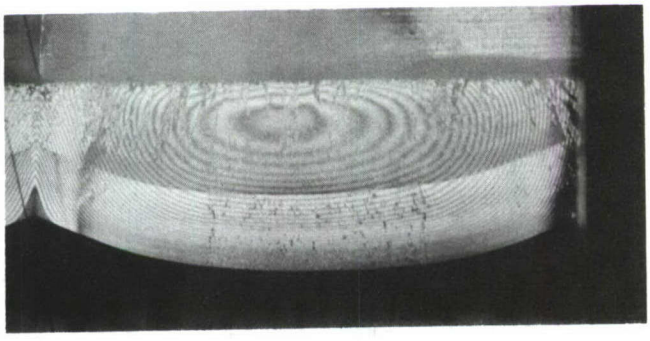

Load = 20 lbs
(K=204 psi $\sqrt{in}$)

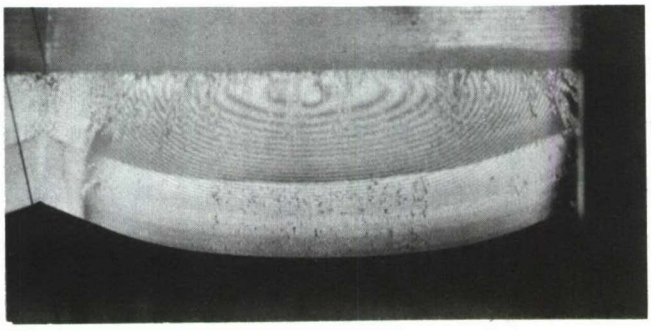

Load = 27.5 lbs
(K=280 psi $\sqrt{in}$)

Fig 16. Specimen 28 Fringe Patterns at Tensile Loads of 17.5, 20 and 27.5 Pounds.

2. With the application of load, the number of fringes increases with the outer fringes moving aft towards the saw cut edge (Fig 15, Load = 5 lbs).
3. The outer-most fringes break at the center of the saw cut edge (Fig 15, Load = 10 lbs).
4. As load increases, the number of broken fringes increases with the outer-most fringe progressing along the saw cut edge towards the free surface. The apparent axes around which the fringes loop move closer together (Fig 15, Load = 15 lbs).
5. The inner-most fringe breaks at the saw cut at about the same load at which the outer fringe reaches the specimen free surface (Fig 16, Load = 17.5 lbs).
6. After reaching the free surface, the outer fringes proceed along the free surface-crack interface towards the crack tip (Fig 16, Load = 20 lbs).
7. The outer fringe reaches the crack tip at the surface (Fig 16, Load = 27.5 lbs).

The actual crack profiles obtained from the fringe patterns are shown in Figs 17 and 18. They show the center profile, surface profile and saw cut profile previously defined. The actual displacements can be obtained from the fringe number (n_f) as

$$\text{Displ} = \frac{2n_f - 1}{4} (2.32 \times 10^{-5} \text{in}) \qquad (6)$$

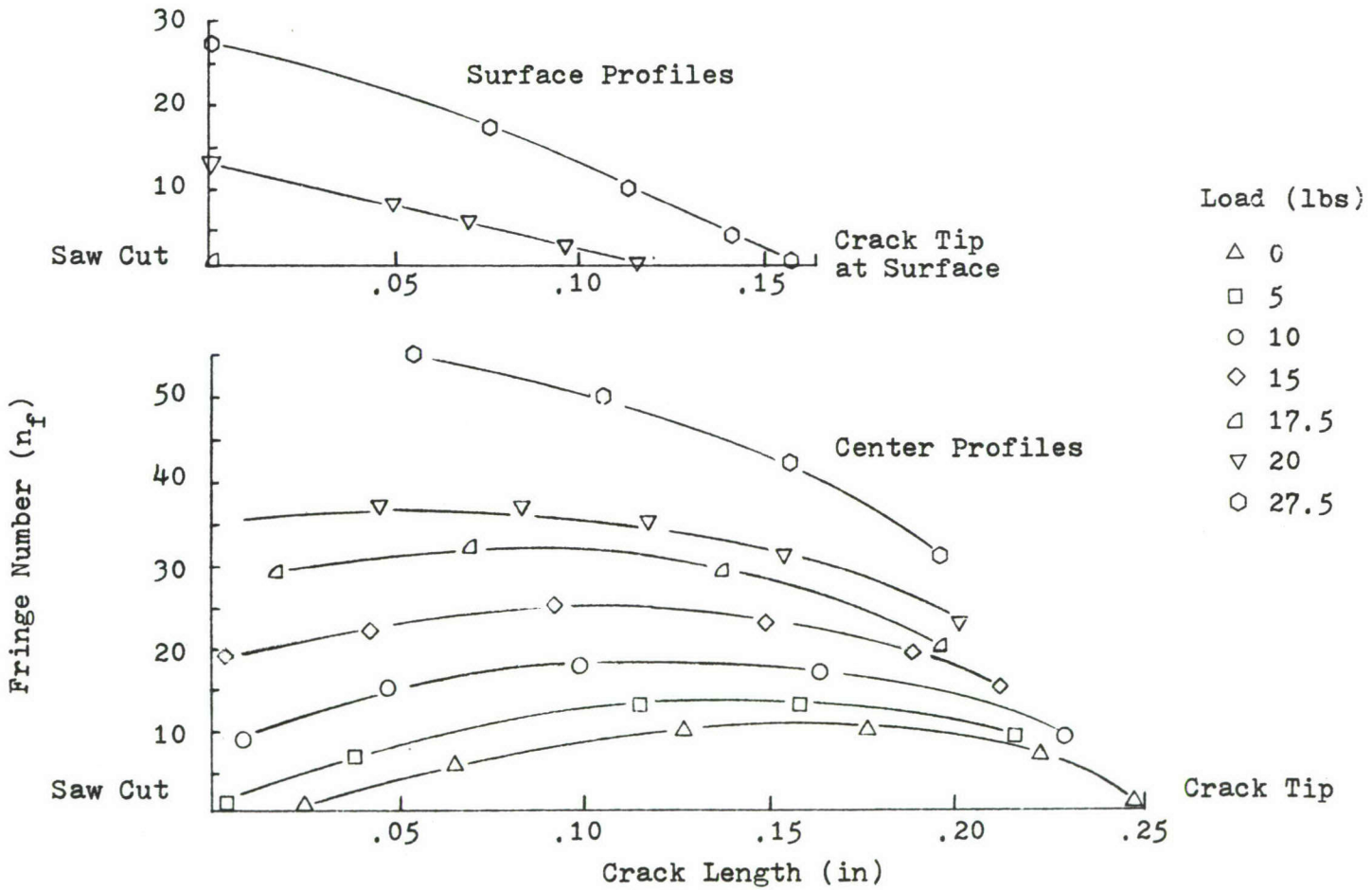

Fig 17. Specimen 28 Fatigue Crack Center and Surface Profiles at Various Tensile Loads.

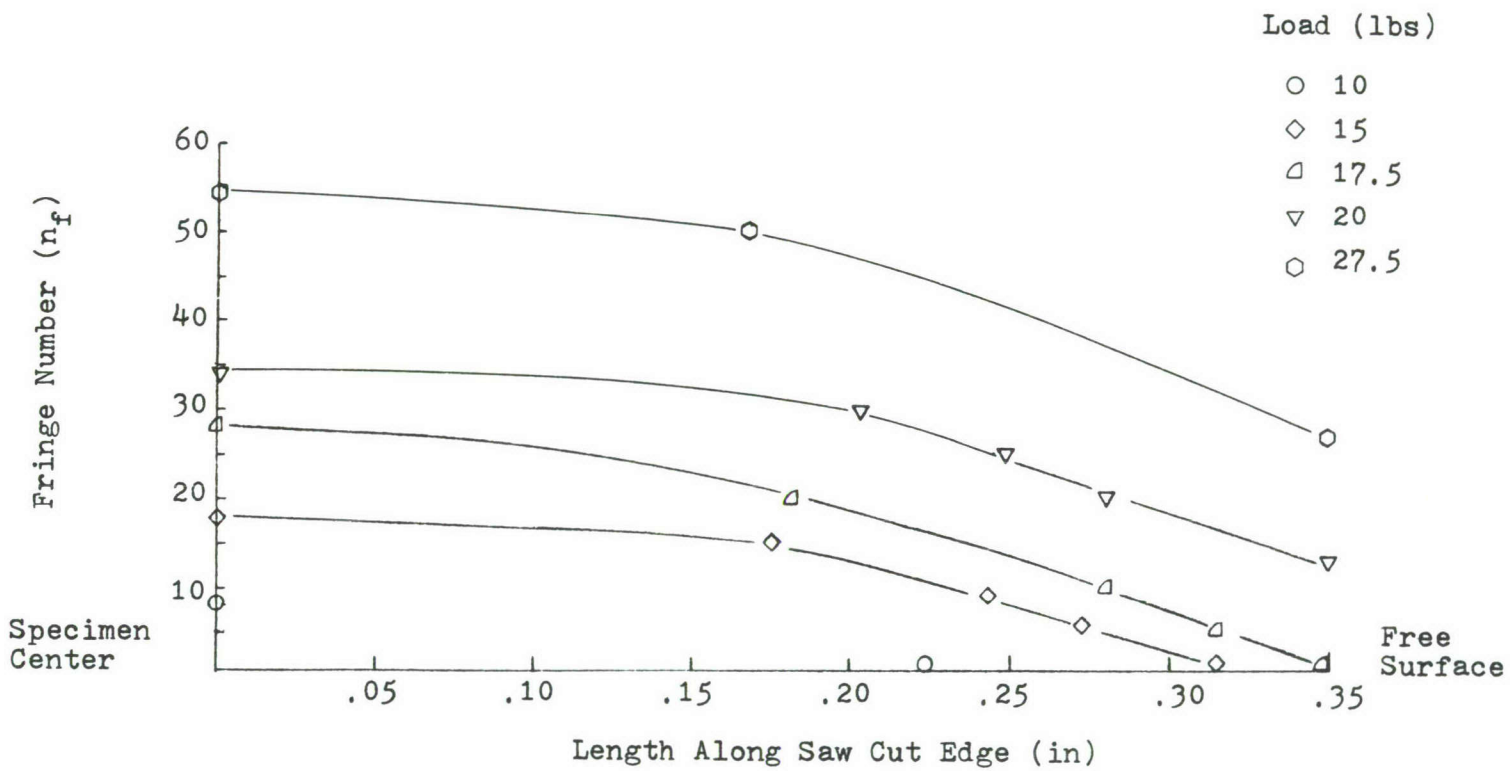

Fig 18. Specimen 28 Fatigue Crack Saw Cut Profiles at Various Tensile Loads.

The following is a discussion of these profiles as well as the fringe patterns themselves.

The closed fringes (not intersecting a specimen surface) at zero load indicate that the crack surfaces are closed at the saw cut edge and the free surface. The crack surfaces are displaced in the center of the specimen, however.

The straight section of each fringe at no load probably is associated with the plane strain conditions in the interior of the specimen. The circular or rounded sections of each fringe probably indicate a transition to the plane stress conditions at the specimen free surface.

As a tensile load is applied, the displacement in the center of the specimen increases proportionally to the number of fringes. In general the center profiles are elliptical with the point of maximum displacement between the crack surfaces moving towards the saw cut edge with increased tensile load. This is indicated by the movement of the innermost fringe center towards the saw cut edge (Fig 15, Load = 10 lbs) and shown in the crack center profiles (Fig 17).

Opening of the crack surfaces at the saw cut edge is indicated first by the outer-most fringe breaking or intersecting the saw cut edge. With increasing tensile load, the crack saw cut profile displacements increase until the entire saw cut edge is open. With the saw cut edge completely open, the point of maximum displacement on the center profile has moved about to the saw cut edge as shown in Fig 16, Load = 17.5 lbs. It is at this load that the crack begins to

open on the free surface at the saw cut edge and progressively moves towards the crack tip.

The above observations agree with the work conducted by Elber (Ref 6). Based on surface crack tip stress-displacement measurements, Elber concluded that a fatigue crack was closed up to some positive stress level. The surface profile observed here is in fact closed up to a certain stress level. The actual value of this stress agrees quite well with the "opening stress" defined by Elber. Working with 2024-T3 aluminum alloy specimens, Elber experimentally determined the opening stress level to be one-half of the maximum previously applied stress for a stress ratio (R) of zero. The value of load at which the first fringe reached the vicinity of the crack tip (Fig 16) was 280 psi $\sqrt{in}$ which is .46 of the maximum baseline value of $K = 600$ psi $\sqrt{in}$.

Elber assumed, however, that his surface observations were characteristic of the crack profile through the thickness of the specimen which is not the case as observed in the present study. Elber's concept of an effective ΔK influencing fatigue crack growth has validity, however. It is reasonable to assume that the energy required to open the crack surfaces at the free surface must reduce the amount of energy available for crack growth during a tensile load cycle.

The concept of "crack closure" therefore must be investigated at two levels: as originally proposed by Elber, the level which is confined to displacements near the crack tip

(10^{-2} inches), and the level observed here along the entire crack-free surface interface.

No information on the crack profile is available prior to the appearance of the first order fringe from the crack tip. The first fringe represents a displacement of approximately 10^{-5} inches. Figure 19 shows two possible profiles from the 10^{-5} inches displacement at the first fringe to the actual crack tip which is approximately 10^{-8} inches characteristic of molecular spacing.

One would assume that the crack growth rates per cycle of two fatigue cracks with the two different profiles shown would be different. It is this level to which Elber refers. The distance of .005 inches from the first fringe to the crack tip was a typical value observed in this study in a no load condition.

(Compression Cycle). Figure 20 shows the corresponding fringe patterns of a CT specimen fatigue crack under zero load and three compressive loads. Again the following will be considered typical to fatigue crack in PMMA grown under similar conditions.

The following sequence of observations was noted with increasing compressive load on the specimen.

1. With the application of a compressive load, the inner fringes move toward the center of the specimen where they disappear. The straight sides move together parallel to each other, eventually merge and disappear while the circular portion of each

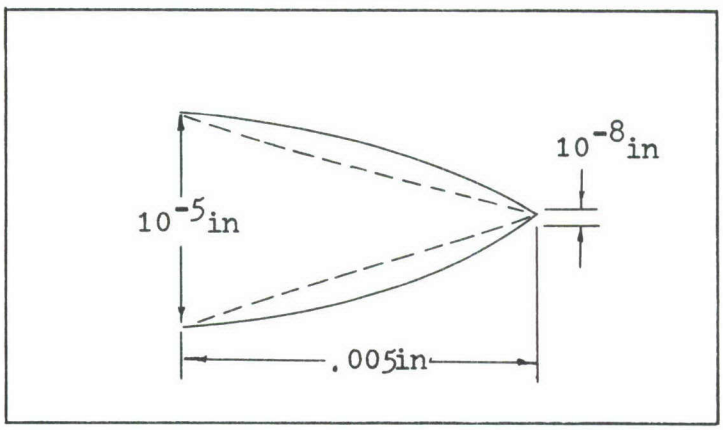

Fig 19. Possible Crack Tip Profiles.

fringe becomes smaller forming a dark circular region and also disappears.

2. There appears to be no shift in the location of the axis around which the circular portion of each fringe is formed.
3. Eventually, all the fringes disappear.

Under the compressive load, the crack surfaces are obviously being forced together. The point of maximum center profile displacements moves towards the crack tip as shown in the center profiles (Fig 21). One distinct difference observed between the tensile and compressive load fringe patterns is the lack of movement in the "axes" under compressive load. The crack surfaces essentially remain parallel to each other when viewed along the Z axis in the plane strain conditions in the interior of the specimen.

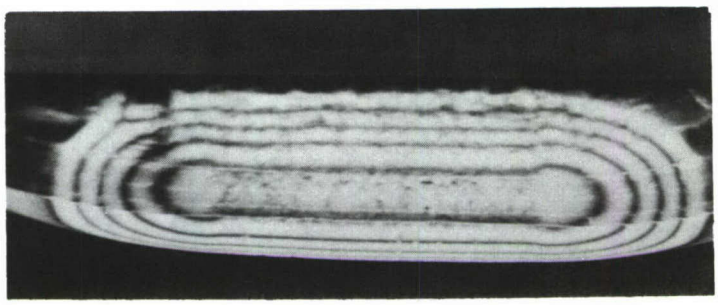

Load = 0 lbs

Crack Tip

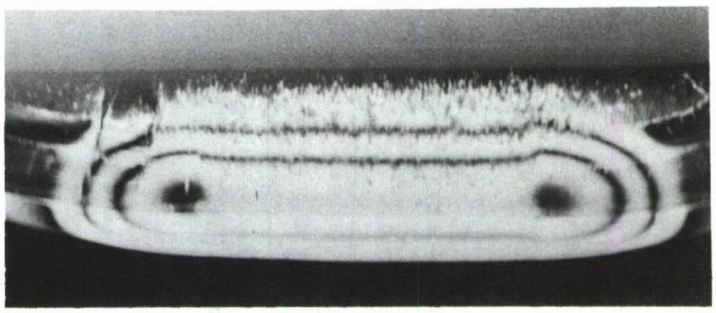

Load = -12.5 lbs

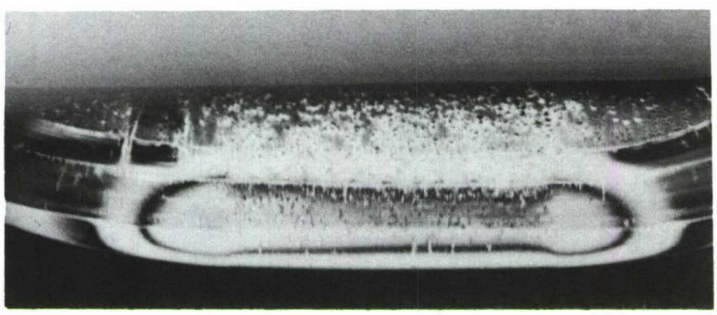

Load = -19.5 lbs

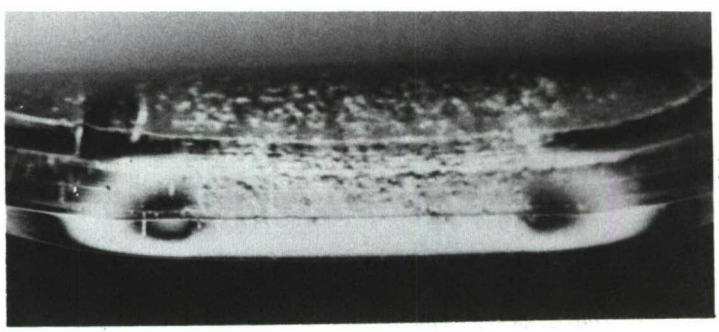

Load = -27.5 lbs

Fig 20. Specimen 22 Fringe Patterns at Compressive Loads of 0, -12.5, -19.5 and -27.5 Pounds.

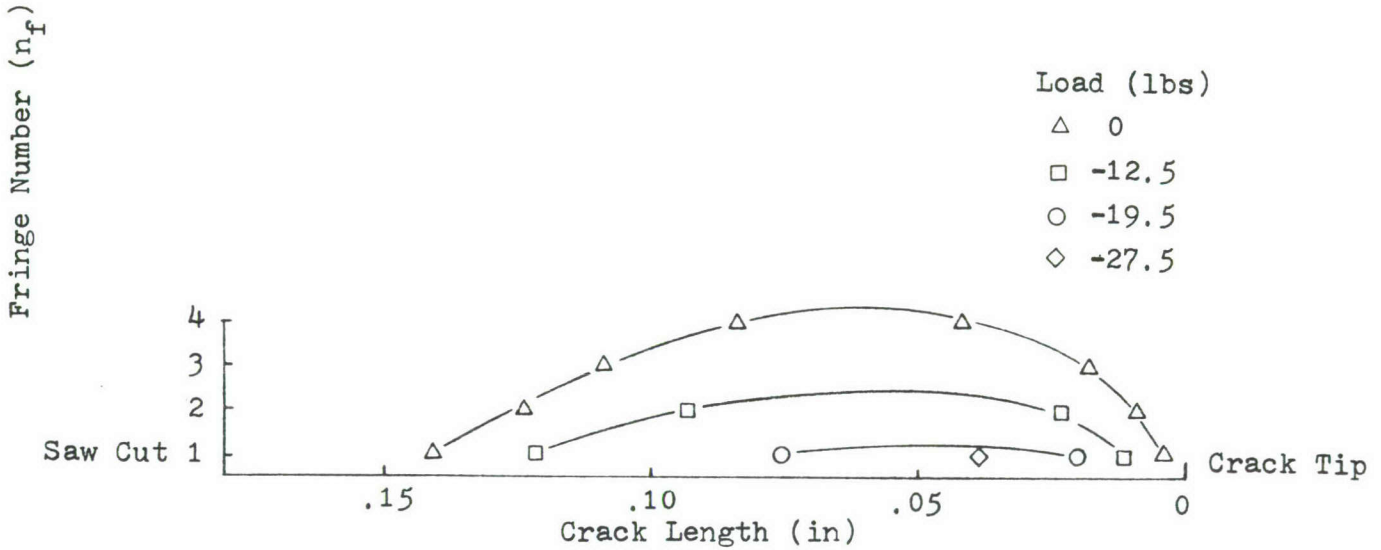

Fig 21. Specimen 22 Fatigue Crack Center Profiles at Various Compressive Loads.

Load History and Crack Length Comparisons. The fringe patterns of fatigue cracks in the CT specimens used in the retardation study were compared to determine the effects of load history and crack length on the number and shapes of the fringes.

Except for three specimens, the only significant difference in the load history of the specimens was the magnitude and number of overloads applied. The majority of the specimens had a baseline $\Delta K = 600$ psi $\sqrt{in}$. In general no conclusive effect due to the overloads could be observed. Fringe patterns obtained prior to and after the application of overloads showed no observable change. One can only conclude that if changes in COD are produced by overloads, they involve changes less than 10^{-5} inches or are occurring too near the crack tip to be resolved at the magnification (10-20X) used.

Specimen 30 was the only specimen which had a significantly different fringe shape. It is shown in Fig 22 along with a typical fringe pattern for the same crack length. Both have four major fringes but specimen 30 has broken fringes indicating that the crack surfaces are displaced at the saw cut. During crack initiation, the higher ΔK's used to start a fatigue crack cause a rough type of fracture surface. In this case the surfaces probably did not properly align (similar to misalignment of gears) and forced the crack surfaces open at the saw cut with no load. This specimen also exhibited peculiar growth characteristics as previously mentioned in the

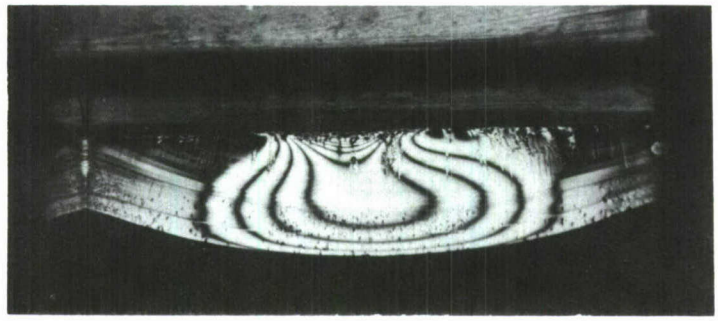

Specimen 30

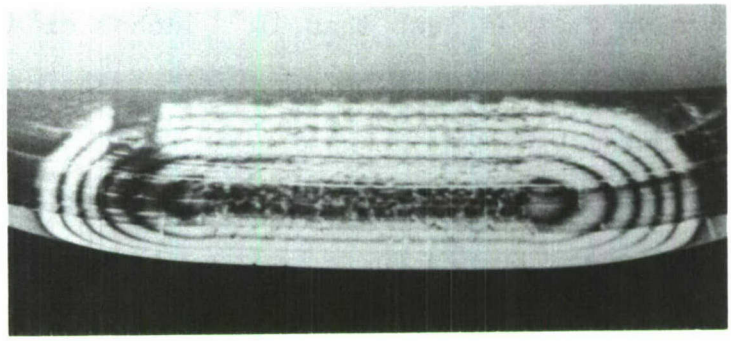

Typical Pattern

Fig 22. Specimen 30 Fringe Pattern
Compared with Typical Pattern.

retardation data section. Continuous crack growth could not be maintained at a ΔK = 450 psi $\sqrt{in}$. The load had to be increased periodically up to ΔK = 500 psi $\sqrt{in}$ to cause any growth at all. During a fatigue load cycle the crack surfaces were not displaced through a complete displacement cycle and this could explain the crack growth behavior. Sustained crack growth was observed on specimen 107R at a ΔK = 450 psi $\sqrt{in}$.

The number of fringes in a fringe pattern and hence the maximum COD of the center profile was observed to be dependent on crack length. At shorter crack lengths (tip to saw cut = .15 inches) the number of fringes was the same. At longer crack lengths (tip to saw cut = .25 inches), the number of fringes varied by 15 to 20 percent. This variation could not be attributed to any particular source and was not considered significant.

Figure 23 shows the center profile of specimen 28 at zero load for three different crack lengths. The distance from the crack tip to the point of maximum COD remained at about the same ratio to the total distance from the crack tip to the saw cut for the three crack lengths.

Relaxation Data. A comparison of fringe patterns obtained from fatigue cracked CT specimens at various time intervals after a specimen was removed from the MTS machine indicated a change in the COD. These changes occurred as a result of the time dependent elastic strain recovery. The resultant fringe pattern was due to the permanent plastic

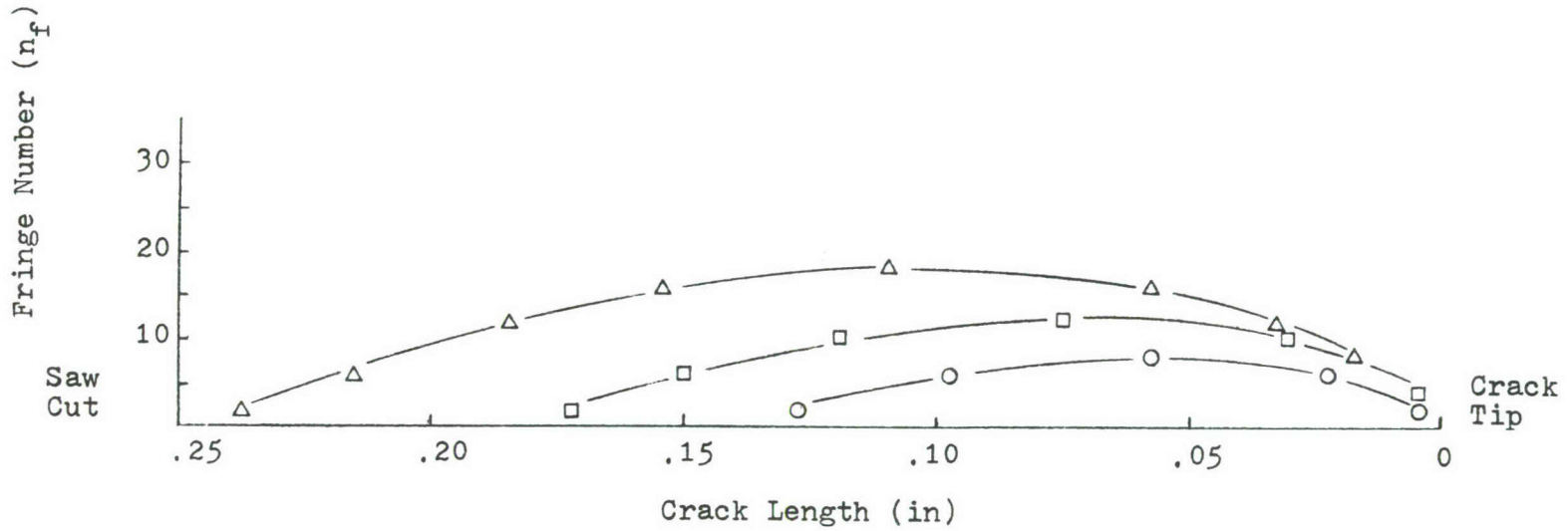

Fig 23. Specimen 28 Zero Load Center Profiles at Three Crack Lengths.

deformations and the resulting internal stresses they generated.

Figures 24 and 25 show examples of the changes occurring in fatigue crack center profiles during stress relaxation. Appendix C contains some of the actual fringe patterns from which the profiles were obtained. In general, a total of one to three fringes were "lost" during a recovery time of 24 hours. This indicated a maximum reduction in COD of 5×10^{-5} inches. The first fringe loss occurred typically in a relaxation time of 5 to 10 minutes. A second fringe loss occured from 15 to 60 minutes. A third fringe loss occurred in 4 to 24 hours only on specimens with longer crack lengths (a = .7 inches). This represented a maximum loss of about 30 percent of the maximum COD observed at that crack length. During the closure of the crack surfaces, the point of maximum COD moved towards the crack tip similar to the effect of a small (2.5 to 5 lb) compressive load.

The effect of an overnight rest period on the baseline crack growth rate could not be determined conclusively because of the scatter in experimental data. A visual mark (similar to one long striation through the thickness of the specimen) usually appeared on the fracture surface, however.

General Discussion. In general the observations contained in this section differed significantly from fringe patterns obtained by Crosley and Sommer (Refs 5, 13) as

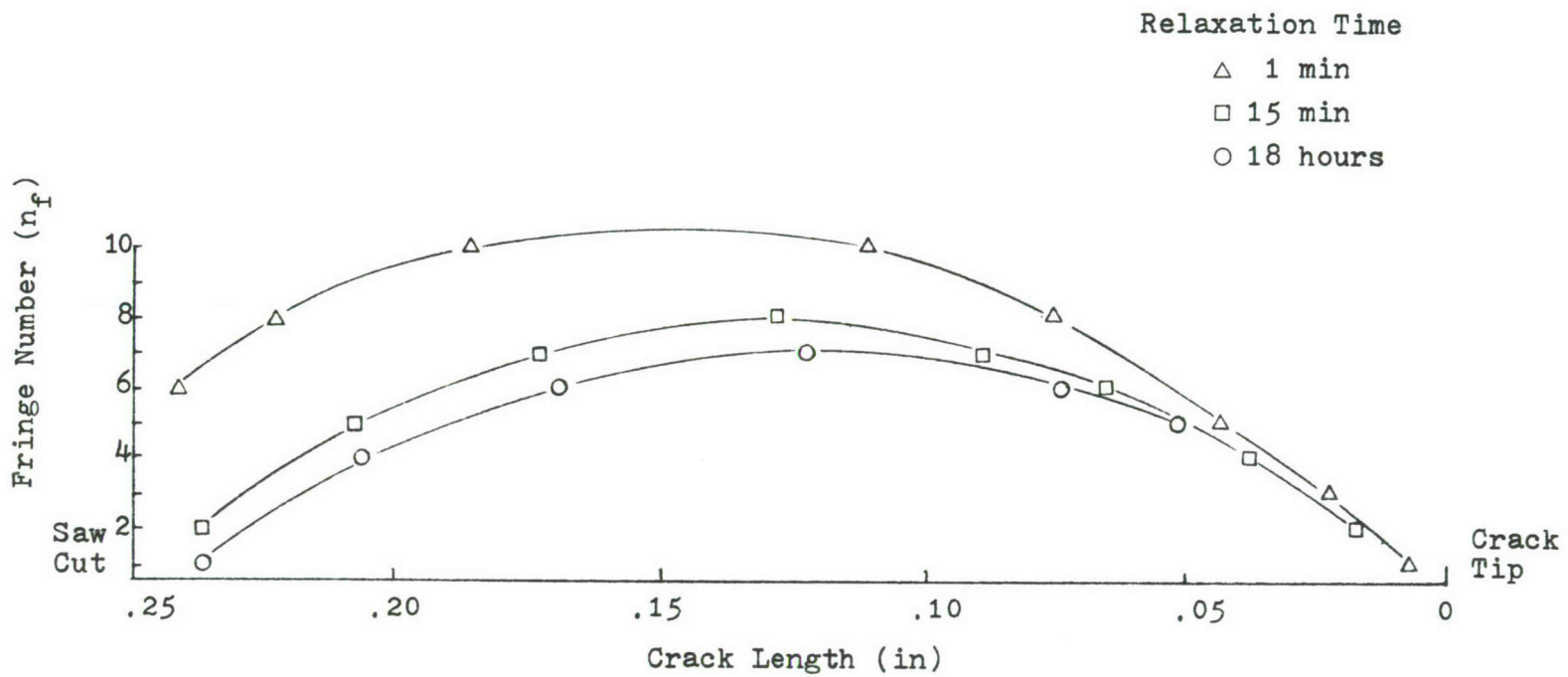

Fig 24. Specimen 20 Fatigue Crack Center Profile with Stress Relaxation.

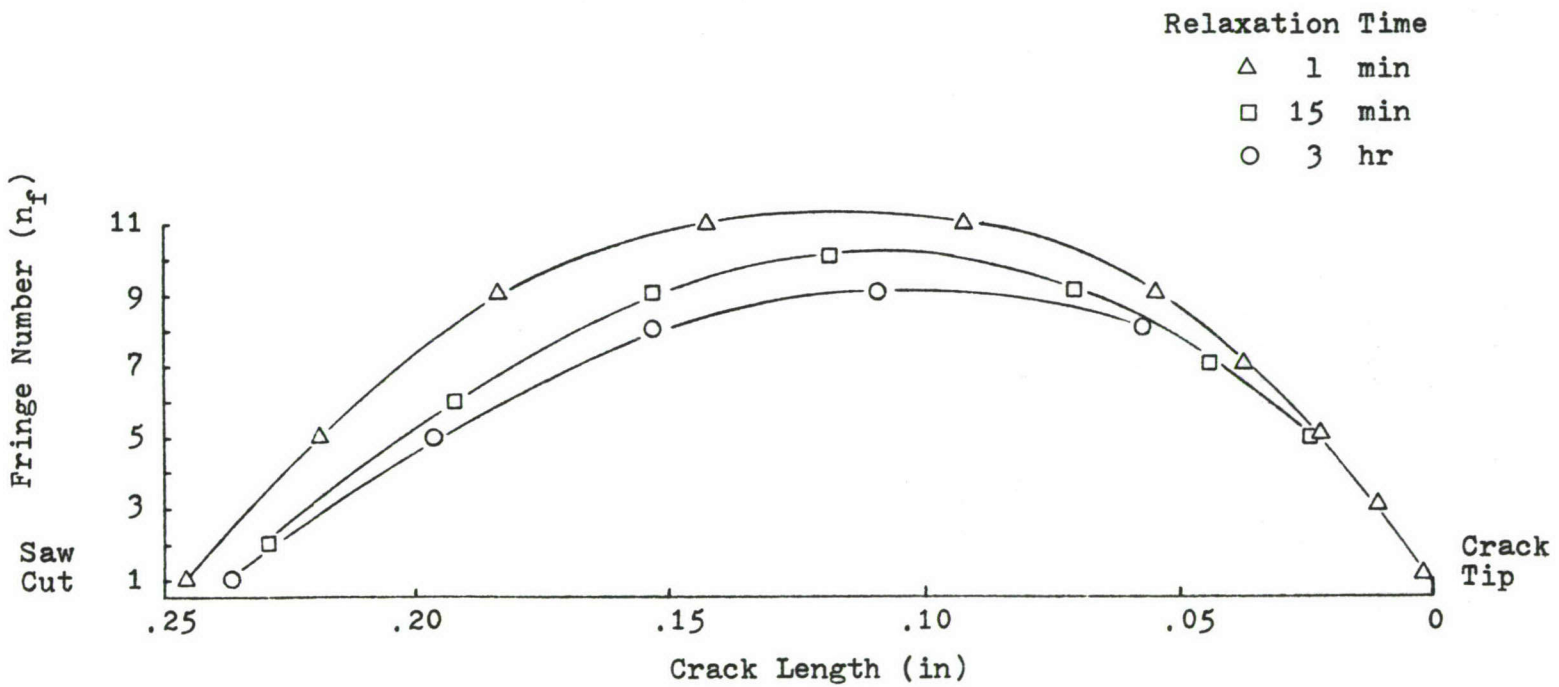

Fig 25. Specimen 28 Fatigue Crack Center Profiles with Stress Relaxation.

might be expected. Their work involved the determination of stress intensity factors by optically measuring COD which then was related to K by the fatigue crack field equations of linear elastic fracture mechanics given in Appendix A.

They measured COD from fringe patterns; however, the cracks in the specimens were not true fatigue cracks. Crosley manufactured his specimens by joining glass beams with an epoxy adhesive and introducing a flaw in the adhesive during the bonding process. The fringe patterns obtained consisted of nearly straight parallel fringes showing little curvature and approximately equally spaced from the crack tip. There are distinct differences between these patterns representative of "ideal" cracks and the "true" fatigue cracks studied here. Therefore one must be careful about drawing valid conclusions characteristic of true fatigue cracks from work involving ideal cracks.

VII. Conclusions and Recommendations

Constant ΔK fatigue crack growth rates in PMMA are affected by peak overloads in much the same manner as in metals; PMMA is therefore considered a suitable material in which to model the fatigue process.

1. It is recommended that additional investigations be made in PMMA to better quantify the overload effects observed in this study. Baseline and overload levels other than those in this study should be considered.
2. Overload effects in other transparent materials such as polycarbonate should be investigated for comparison with the observations in this study. Emphasis should be placed on isolating effects which are peculiar to the material and those which are characteristic to the fatigue process in general.

The true fatigue cracks observed in this study are open in the interior of unloaded CT specimens but the crack surfaces remain closed at the free surfaces up to some positive load level. This opening load agrees numerically with the opening stress level as predicted by the Elber closure concept.

Interferometry proved to be a valuable technique by which to obtain data concerning the fatigue process.

3. It is recommended that further investigations be performed to further quantify true fatigue crack surface displacements, especially near the crack tip, during cyclic loads.
4. The specific procedure used in this study should be modified by using a monochromatic light source with a shorter wavelength, such as a mercury violet light source, to provide a more precise means with which to measure COD changes. Microscopic photography should be used to provide better resolution of fringes near the crack tip.

Bibliography

1. Adams, N.J.I. "Fatigue Crack Closure at Positive Stresses." Paper presented at the Symposium on Fracture and Fatigue, George Washington University, Washington, D.C. (3-5 May 1972).

2. Arad, S., J.C. Radon and L.E. Culver. "Fatigue Crack Propagation in Polymethylmethacrylate; the Effect of the Mean Value of Stress Intensity Factor." Journal Mechanical Engineering Science, 13:75-81 (1971).

3. Borduas, H.E., L.E. Culver and D.J. Burns. "Fracture-Mechanics Analysis of Fatigue-Crack Propagation in Polymethylmethacrylate." Journal of Strain Analysis, 3:193-199 (1968).

4. Corbly, D.M. and P.F. Packman. "On the Influence of Single and Multiple Peak Overloads on Fatigue Crack Propagation in 7075-T6511 Aluminum." Paper presented at The Symposium on Fracture and Fatigue, George Washington University, Washington, D.C. (3-5 May 1972).

5. Crosley, P.B., S. Mostovoy and E.J. Ripling. "An Optical-Interference Method for Experimental Stress Analysis of Cracked Structures." Engineering Fracture Mechanics, 3:421-433 (Dec 1971).

6. Elber, Wolf. "The Significance of Fatigue Crack Closure." Damage Tolerance in Aircraft Structures, ASTM STP486, American Society for Testing and Materials, 230-242 (1971).

7. Elber, Wolf. "Fatigue Crack Closure Under Cyclic Tension." Engineering Fracture Mechanics, 2:37-45 (1970).

8. Grandt, A.F., Jr. and G.M. Sinclair. "Stress Intensity Factors for Surface Cracks in Bending." Stress Analysis and Growth of Cracks, Proceedings of the 1971 National Symposium on Fracture Mechanics, Part I. ASTM STP 513, American Society for Testing and Materials, 37-58 (1972).

9. Hertzberg, R.W., H. Nordberg and J.A. Manson. "Fatigue Crack Propagation in Polymeric Materials." Journal of Materials Science, 5:521-526 (1970).

10. James, L.A. "Fatigue-Crack Growth in Type 304 Stainless Steel Weldments at Elevated Temperature." Paper prepared for presentation at the ASTM Symposium on Fatigue at Elevated Temperatures, Storrs, Connecticut (18-22 June 1972).

11. Mukherjee, B. and D.J. Burns. "Fatigue-Crack Growth in Polymethylmethacrylate." Experimental Mechanics, 11:433-439 (Oct 1971).

12. Mukherjee, B., L.E. Culver and D.J. Burns. "Growth of Part-through and Through-thickness Fatigue Cracks in Sheet Glassy Plastics." Experimental Mechanics, 90-96 (Feb 1969).

13. Sommer, E. "An Optical Method for Determining the Crack-Tip Stress Intensity Factor." Engineering Fracture Mechanics, 1: 705-718 (1970).

14. Theocaris, P.S. "Local Yielding Around a Crack Tip in Plexiglas." ASME Paper No 70-APM-BB

15. Tetelman, A.S. and A.J. McEvily, Jr. Fracture of Structural Materials. New York: John Wiley and Sons, Inc., 1967.

16. Vroman, G.A. "Analytical Prediction of Crack Growth Retardation Using a Residual Stress Intensity Concept." Los Angeles Division, North American Rockwell Paper, May 1971.

17. Von Euw, E.F.J., R.W. Hertzberg and R. Roberts "Delay Effects in Fatigue Crack Propagation." Paper presented at the Fifth National Symposium on Fracture Mechanics, University of Illinois, Urbana, Illinois (31 Aug-2 Sept 1971).

18. Watts, N.H. and D.J. Burns. "Fatigue Crack Propagation in Polymethymethacrylate." Polymer Engineering and Science, 7:90-93 (April 1967).

19. Wheeler, O.E. "Spectrum Loading and Crack Growth" ASME Paper No. 71-MET-X.

20. Willenburg, J., R.M. Engle and H.A. Wood. "A Crack Growth Retardation Model Using an Effective Stress Concept." TM-71-1-FBR, Air Force Flight Dynamics Laboratory, (Jan 1971).

21. Paris, P.C. and F. Erdogen. "A Critical Analysis of Crack Propagation Laws." Journal of Basic Engineering, Transaction at ASME. Series D, 85:528-539 (1963).

Appendix A

Linear Elastic Crack Field Equations

The following equations relate the stresses and displacements around the tip of a fatigue crack (as oriented) to the stress intensity factor at the crack tip. The stress intensity factor is a function of the far field applied stress, the body geometry and the crack length.

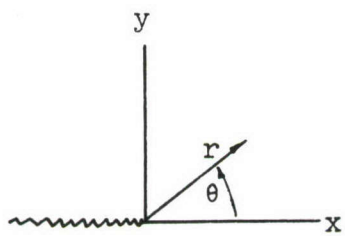

Fatigue Crack

$$\sigma_x = \frac{K_I}{\sqrt{2\pi r}} \cos\left(\frac{\theta}{2}\right)\left[1-\sin\left(\frac{\theta}{2}\right)\cos\left(\frac{3\theta}{2}\right)\right]$$

$$\sigma_y = \frac{K_I}{\sqrt{2\pi r}} \cos\left(\frac{\theta}{2}\right)\left[1+\sin\left(\frac{\theta}{2}\right)\cos\left(\frac{3\theta}{2}\right)\right]$$

$$\sigma_{xy} = \frac{K_I}{\sqrt{2\pi r}} \cos\left(\frac{\theta}{2}\right)\left[\sin\left(\frac{\theta}{2}\right)\cos\left(\frac{3\theta}{2}\right)\right]$$

$$u_x = \frac{K_I\sqrt{r/2\pi}}{2G} \cos\left(\frac{\theta}{2}\right)\left[\alpha - 1 + 2\sin^2\left(\frac{\theta}{2}\right)\right]$$

$$u_y = \frac{K_I\sqrt{r/2\pi}}{2G} \sin\left(\frac{\theta}{2}\right)\left[\alpha + 1 - 2\cos^2\left(\frac{\theta}{2}\right)\right]$$

$\alpha = 3-4\nu$ plane strain

$= \frac{3-\nu}{1+\nu}$ plane stress

G = Shear modulus

ν = Poisson's Ratio

The above equations are generally considered valid for $r < a/10$ (a being crack length). Of course, they do not give valid results near the crack tip if non-linear (plastic) effects are permitted.

By obtaining crack opening displacements (u_y at $\theta = \pi$), the theoretical value of K can be solved for from the (u_y) equation. The value of K may not be the correct value for a true fatigue crack but, it would provide a first order approximation.

Appendix B

Tensile Cycle Fringe Patterns

The following two series of photographs (Figs 26 to 29) show the similarity of fringe pattern changes during a tensile load cycle. Both specimens (20 and 27) have a crack length of .7 inches (tip to saw cut = .45 inches).

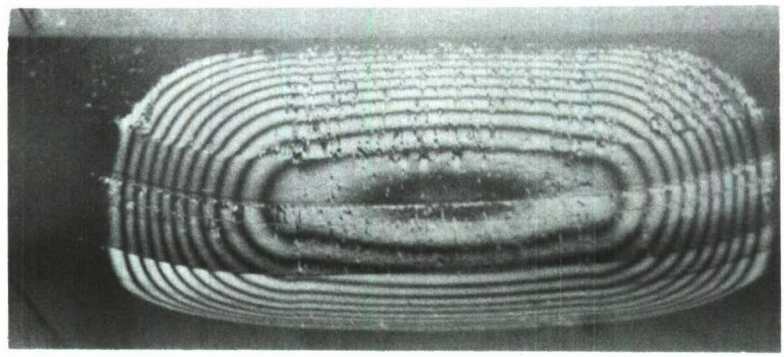

Load = 2.5 lbs

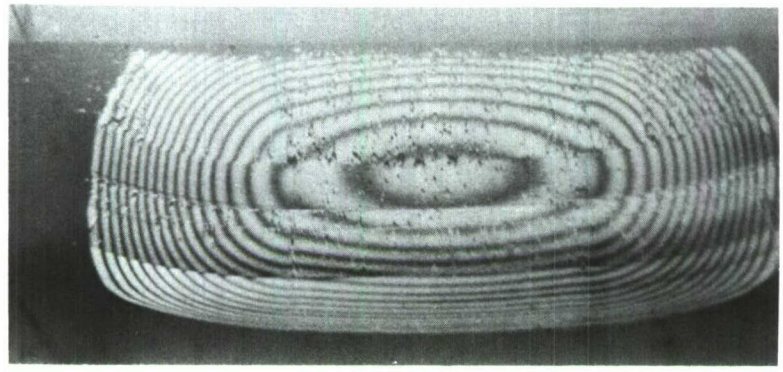

Load = 7.5 lbs

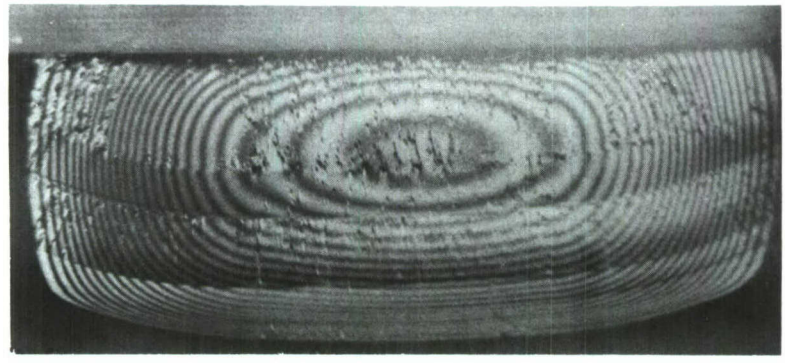

Load = 12.5 lbs

Fig 26. Specimen 20 Fringe Patterns at Tensile Loads of 2.5, 7.5, and 12.5 Pounds.

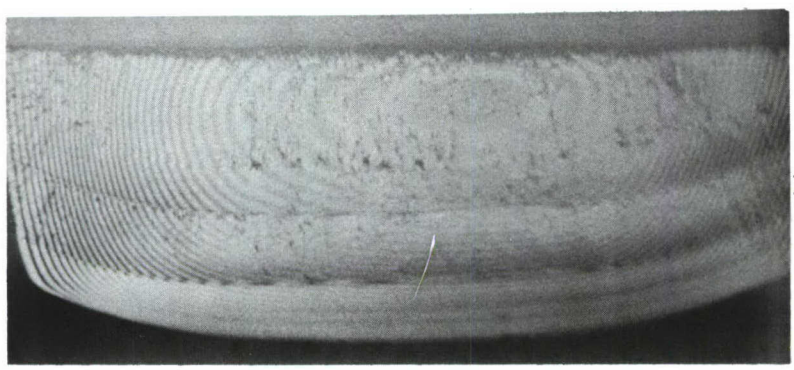

Load = 17.5 lbs

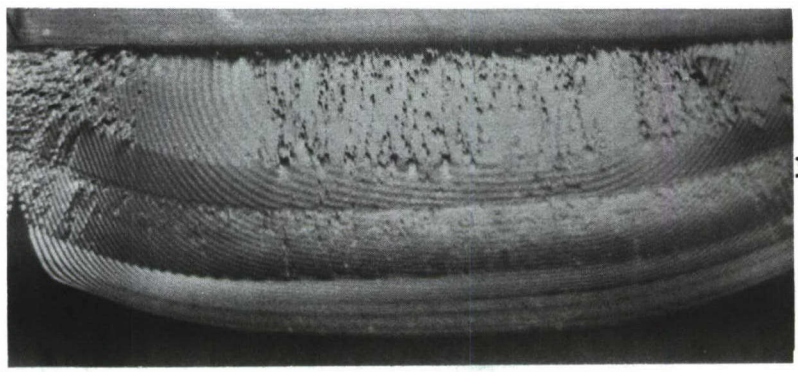

Load = 22.5 lbs

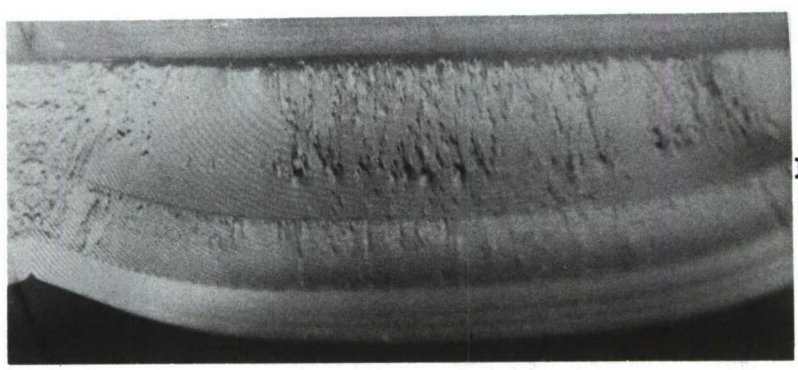

Load = 27.5 lbs

Fig 27. Specimen 20 Fringe Patterns at Tensile Loads of 17.5, 22.5, and 27.5 Pounds.

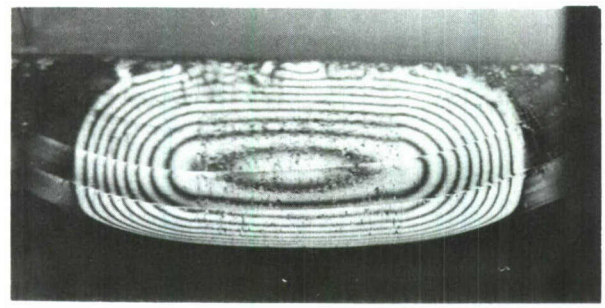

Load = 0 lbs

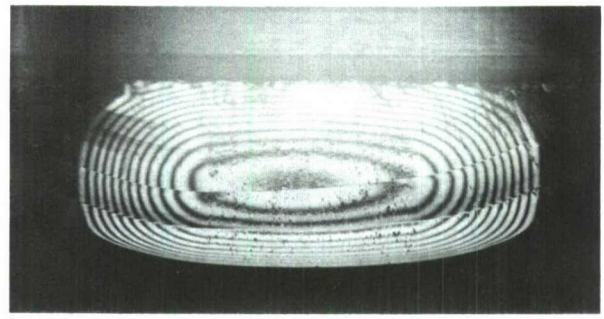

Load = 5 lbs

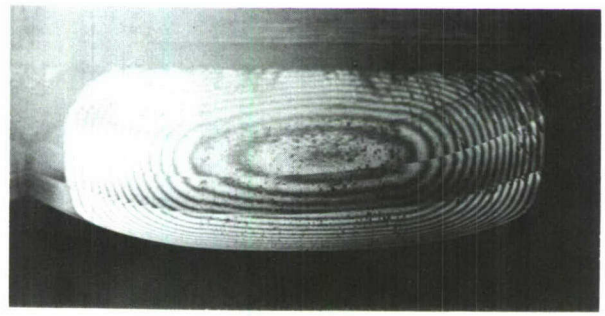

Load = 10 lbs

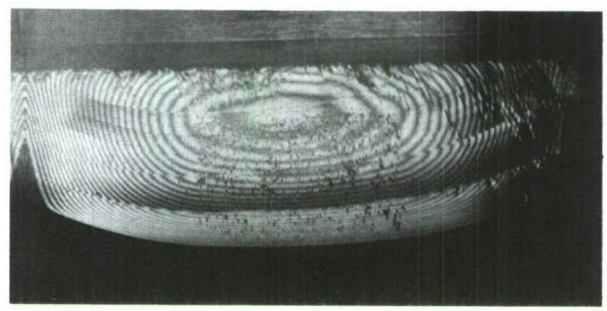

Load = 17.5 lbs

Fig 28. Specimen 27 Fringe Patterns at Tensile Loads of 0, 5, 10, and 17.5 Pounds.

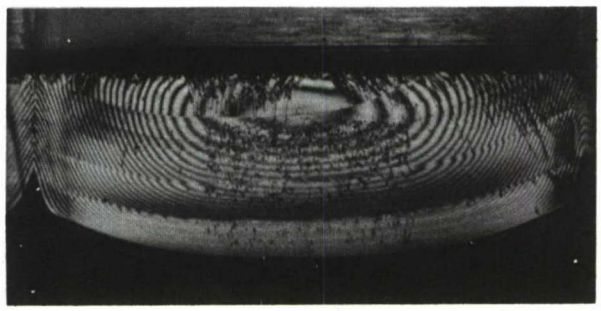

Load = 20 lbs

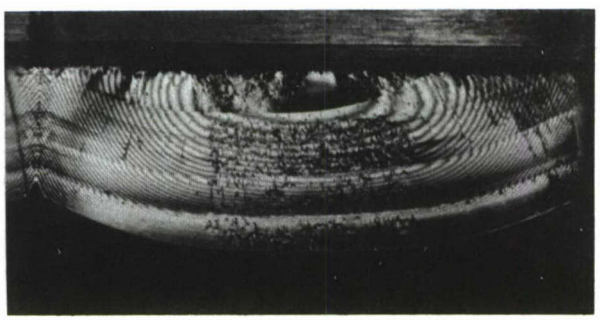

Load = 22.5 lbs

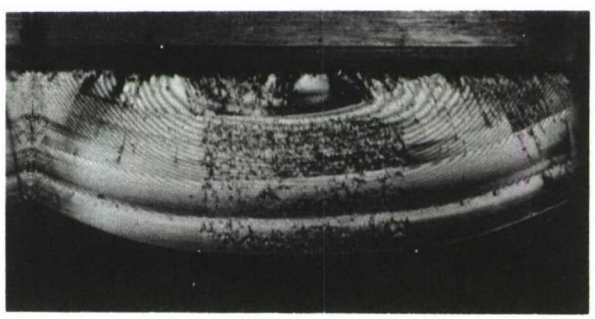

Load = 27.5 lbs

Fig 29. Specimen 27 Fringe Patterns at Tensile Loads of 20, 22.5, and 27.5 Pounds.

Appendix C

Stress Relaxation Fringe Patterns

Figure 30 shows the fringe patterns of a fatigue crack at various relaxation times. The fatigue crack is open along the saw cut one minute after removal from the MTS machine. The crack surfaces are closed at the saw cut after 15 minutes.

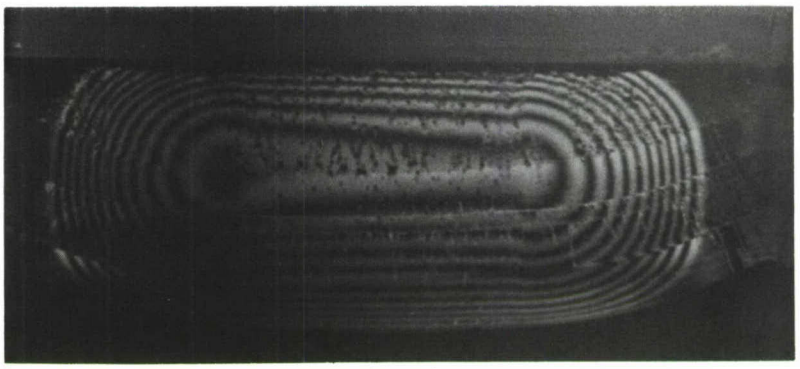

1 min

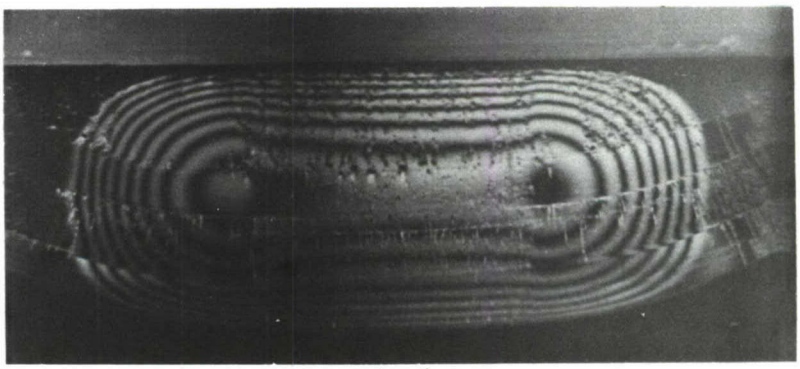

15 min

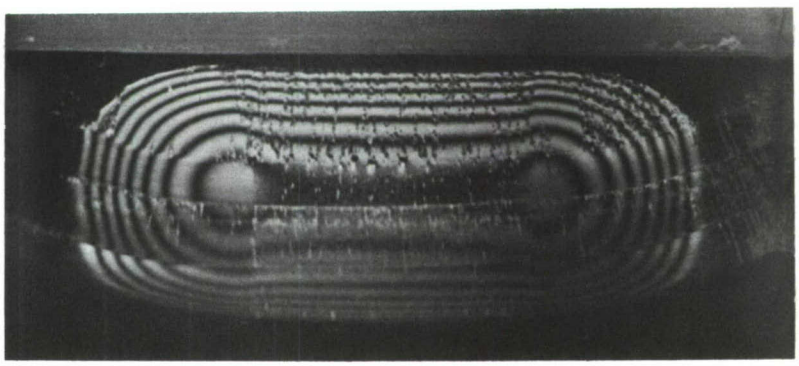

18 hours

Fig 30. Specimen 20 Fringe Pattern Changes with Stress Relaxation.

Unclassified

Security Classification

DOCUMENT CONTROL DATA - R & D

(Security classification of title, body of abstract and indexing annotation must be entered when the overall report is classified)

1. ORIGINATING ACTIVITY *(Corporate author)* Air Force Materials Laboratory Wright Patterson AFB, Ohio 45433	2a. REPORT SECURITY CLASSIFICATION Unclassified 2b. GROUP

3. REPORT TITLE

EXPERIMENTAL STUDY OF FATIGUE CRACK PROPAGATION AND RETARDATION USING POLYMETHYLMETHACRYLATE

4. DESCRIPTIVE NOTES *(Type of report and inclusive dates)*

Technical Report (AFIT Thesis)

5. AUTHOR(S) *(First name, middle initial, last name)*

Francis J. Pitoniak, Captain, USAF
Air Force Institute of Technology

6. REPORT DATE	7a. TOTAL NO. OF PAGES	7b. NO. OF REFS
November 1972	71	21

8a. CONTRACT OR GRANT NO. N/A b. PROJECT NO. 7353 c. Task 735309 d.	9a. ORIGINATOR'S REPORT NUMBER(S) AFML-TR-72-235 9b. OTHER REPORT NO(S) *(Any other numbers that may be assigned this report)* AFIT Thesis# GAM/MC-73-2

10. DISTRIBUTION STATEMENT

Approved for public release; distribution unlimited

11. SUPPLEMENTARY NOTES	12. SPONSORING MILITARY ACTIVITY
	N/A

13. ABSTRACT

Fatigue cracks were grown in compact tension specimens of polymethylmethacrylate, a transparent polymer which was used as a model for metals. Various peak overloads applied to the constant ΔK baselines used produced changes in the baseline load crack growth rates. One thousand overloads of ΔK = 600 psi $\sqrt{in}$ produced a reduced or "retarded" growth rate followed by a net baseline growth rate increase. Five overloads to ΔK = 900 psi $\sqrt{in}$ on a baseline load level of ΔK = 450 psi $\sqrt{in}$ produced apparent crack arrest.

A study of the monochromatic light interference fringe patterns emanating from the fatigue cracks at zero load indicated that the crack surfaces were closed along the saw cut edge and on the free surface of the specimens. The crack surfaces were displaced in the interior of the specimen at zero load. Measurement of the crack opening displacements from the fringe patterns indicated that the crack surfaces opened on the free surface at approximately half the baseline load level for a stress ratio of approximately zero. This is in agreement with the Elber crack closure concept.

DD FORM 1 NOV 65 1473

Unclassified

Security Classification

14. KEY WORDS	LINK A		LINK B		LINK C	
	ROLE	WT	ROLE	WT	ROLE	WT

☆U.S.Government Printing Office: 1973 — 759-490/323